JOURNAL OF VIROLOGY, Aug. 2002, p. 8383–8399 Vol. 76, No. 16
0022-538X/02/$04.00+0 DOI: 10.1128/JVI.76.16.8383–8399.2002

Kaposi's Sarcoma-Associated Herpesvirus-Induced Upregulation of the c-*kit* Proto-Oncogene, as Identified by Gene Expression Profiling, Is Essential for the Transformation of Endothelial Cells

Ashlee V. Moses,[1]* Michael A. Jarvis,[1] Camilo Raggo,[1] Yolanda C. Bell,[3] Rebecca Ruhl,[1] B. G. Mattias Luukkonen,[3] Diana J. Griffith,[4] Cecily L. Wait,[4] Brian J. Druker,[4] Michael C. Heinrich,[4] Jay A. Nelson,[1,2] and Klaus Früh[1]*

Vaccine and Gene Therapy Institute[1] and Department of Molecular Microbiology and Immunology,[2] Oregon Health and Science University, and Division of Hematology and Medical Oncology, Oregon Health and Science University and Portland Veterans Affairs Medical Center,[4] Portland, Oregon 97201, and R. W. Johnson Pharmaceutical Research Institute, San Diego, California 92121[3]

Received 10 April 2002/Accepted 3 May 2002

Kaposi's sarcoma (KS), the most frequent malignancy afflicting AIDS patients, is characterized by spindle cell formation and vascularization. Infection with KS-associated herpesvirus (KSHV) is consistently observed in all forms of KS. Spindle cell formation can be replicated in vitro by infection of dermal microvascular endothelial cells (DMVEC) with KSHV. To study the molecular mechanism of this transformation, we compared RNA expression profiles of KSHV-infected and mock-infected DMVEC. Induction of several proto-oncogenes was observed, particularly the receptor tyrosine kinase c-*kit*. Consistent with increased c-Kit expression, KHSV-infected DMVEC displayed enhanced proliferation in response to the c-Kit ligand, stem cell factor (SCF). Inhibition of c-Kit activity with either a pharmacological inhibitor of c-Kit (STI 571) or a dominant-negative c-Kit protein reversed SCF-dependent proliferation. Importantly, inhibition of c-Kit signal transduction reversed the KSHV-induced morphological transformation of DMVEC. Furthermore, overexpression studies showed that c-Kit was sufficient to induce spindle cell formation. Together, these data demonstrate an essential role for c-Kit in KS tumorigenesis and reveal a target for pharmacological intervention.

Kaposi's sarcoma (KS)-associated herpesvirus (KSHV) (or human herpesvirus 8) is consistently associated with all epidemiologic forms of KS and is recognized as the etiologic agent of the disease (15, 27). Within the KS lesion, KSHV infects the spindle-shaped cells that characterize the tumor as well as their endothelial cell precursors (15, 62, 100). The majority of infected cells harbor the KSHV genome in a latent form, with a small percentage entering a lytic cycle and producing infectious virus (82, 102, 116).

KSHV genes with the potential to deregulate cellular growth have been described previously. Several of these genes have homology to human oncogenes and growth factors or transforming genes of other oncogenic herpesviruses, while others are unique to KSHV (33). KSHV regulatory gene products include homologs of cellular cytokines (viral interleukin-6 [vIL-6]) (70) and chemokines (viral macrophage inflammatory protein I [vMIP-I]/open reading frame K4 [ORF K4], vMIP-II/ORF K6, and vMIP-III/ORF K4.1) (13); the antiapoptotic proteins viral B-cell lymphoma 2 [vBCL-2]/ORF16 (30) and viral FLICE-inhibitory protein [vFLIP]/ORF71 (106); an inhibitor of interferon signaling (viral interferon regulatory factor [vIRF]/ORF K9) (44); a cyclin D homolog (viral cyclin [vCYC]/ORF72) (28); a viral G-protein-coupled receptor (vGCR) with homology to the IL-8 receptor (vGCR/ORF74) (9, 23); the viral protein Kaposin (ORF K12) (116), which has been shown to have transforming ability (73); and the latent nuclear antigen (LANA/ORF73), which modulates cellular transcription (84). Interestingly, three of these gene products, LANA, vFLIP and vCYC are thought to constitute the latent gene expression program in KSHV and are consistently expressed in all virally infected cells in KS, primary effusion lymphoma (PEL), and multicentric Castleman's disease (MCD) (34, 36, 102). Other gene products such as the vGCR and vIL-6 are expressed in a minority of infected tumor cells in vivo (20, 47, 99). While lytic infection may not be compatible with transformation, lytic gene products are thought to have important paracrine effects on adjacent latently infected or uninfected cells that are vital for lesion formation. In addition, viral gene expression patterns may be tumor or stage specific, and some early lytic genes may be expressed for an extended period of time in the absence of a complete replication cycle. Thus, KSHV encodes an arsenal of proteins that could conceivably induce and/or maintain KS lesions. Despite this recognition, the mechanisms of virus-induced oncogenesis remain unclear.

In vitro studies with KSHV were initially performed using PEL cell lines established from PEL tumors that comprise a rare form of AIDS-associated B-cell lymphoma (7, 14, 22). PEL cells stably maintain KSHV episomes, and lytic viral replication can be induced in a significant percentage (>30%) of cells following treatment with phorbol esters or sodium butyrate. PEL cells have thus proved invaluable for mapping and

* Corresponding author. Mailing address: 505 NW 185th Ave., Beaverton, OR 97006. Phone: (503) 418-2735. Fax: (503) 418-2701. E-mail for Klaus Früh: fruehk@ohsu.edu. E-mail for Ashlee V. Moses: mosesa@ohsu.edu.

characterizing the KSHV genome (75, 86, 93, 103) and have provided a source of infectious KSHV for infection of other cell types. In addition, DNA array analysis of PEL cells has been used to map the transcription program of KSHV (57, 78). Endothelial cells are, however, a more relevant cell type in which to study KS pathogenesis, since they are the likely precursors of KS spindle cells (11, 90, 91, 96). Interestingly though, cells cultured from KS tumors do not maintain the KSHV genome (3, 4), and the early consequences of cellular transformation are inaccessible via the study of fully transformed tumor cells. In vitro endothelial cell models of KSHV infection thus provide the most useful systems with which to dissect the role of KSHV in KS spindle cell development and growth, but development of such systems has proved to be challenging. To date several endothelial-based models of KSHV infection have been described (31, 42, 60, 71). Each model has unique characteristics and has thus contributed distinct but complementary information to the field. The system described by Flore et al. highlights the role played by paracrine signaling, since only a percentage of cells harbor the viral genome (42). Other systems describe endothelial cell cultures in which latent infection predominates, but only that characterized by Ciufo et al. utilizes primary cells (31). The other models utilize dermal microvascular endothelial cells (DMVEC) first immortalized by human papillomavirus (HPV) gene products (71) or telomerase (60), since primary endothelial cells have a limited life span in vitro. While prior immortalization precludes a strict analysis of the effect of the virus on cell survival, it does allow for a long-term maintenance of infected cells and the robust growth of mock-infected controls.

To identify the molecular mechanisms involved in KSHV-induced endothelial cell transformation, we applied gene expression profiling by cDNA arrays to KSHV-infected DMVEC. We chose the KSHV-permissive immortalized DMVEC system as previously described (71) for the gene profiling studies since this system allows us to generate age- and passage-matched KSHV- and mock-infected cells. This system duplicates many features of a natural infection of KS spindle cells. For example, KSHV remains latent in the majority of DMVEC infected in vitro, with virus in approximately 2% of cells entering the lytic replication cycle. In addition, latently infected DMVEC change from cobblestone to spindle morphology and exhibit features of transformation including loss of contact inhibition and growth in soft agar. Immortalization results in a very robust and reproducible infection system. To identify cellular genes that may contribute to KSHV-induced transformation, we used cDNA arrays for gene expression profiling of age- and passage-matched KSHV-infected and uninfected DMVEC. Induction of several proto-oncogenes was observed, including the receptor tyrosine kinase c-*kit*. c-*kit* induction was confirmed by quantitative real-time PCR analysis, while immunofluorescent staining confirmed upregulation of the c-Kit protein in primary as well as immortalized KSHV-infected DMVEC. Importantly, infected DMVEC displayed a ligand-dependent growth advantage that could be eliminated by STI 571 (Gleevec) a pharmacological inhibitor of c-Kit activity (50). Moreover, we show that c-Kit was sufficient for induction of the transformed phenotype in DMVEC and that specific inhibition of c-Kit signaling reversed this phenotype in KSHV-infected cells. Abnormal c-Kit signaling due to receptor overexpression and/or constitutive activation has been implicated in a variety of cancers (12, 63). Our results suggest that KSHV may contribute to KS development through modulation of c-Kit expression and function and, further, identify this cellular proto-oncogene as a novel target for therapeutic intervention.

MATERIALS AND METHODS

Derivation of KSHV-infected DMVEC. KSHV-infected DMVEC were established as previously described in detail (71). Briefly, DMVEC immortalized by retroviral expression of the E6 and E7 genes of HPV type 16 (DMVEC) were infected with KSHV derived from the supernatant of tetradecanoyl phorbol acetate-stimulated BCBL-1 cells. DMVEC were maintained in endothelial-SFM (GIBCO BRL, Gaithersburg, Md.) supplemented with 10% human AB serum (HS; Sigma, St Louis, Mo.), penicillin (100 U/ml), streptomycin (100 μg/ml), 2 mM glutamine, endothelial cell growth supplement (25 μg/ml; Becton Dickinson, Bedford, Mass.), heparin (40 μg/ml; Sigma) and G418 (200 μg/ml; GIBCO BRL). The BCBL-1 cell line was obtained through the AIDS Research and Reference Reagent Program, Division of AIDS, National Institute of Allergy and Infectious Diseases, National Institutes of Health (contributed by Michael McGrath and Don Ganem) and cultured in RPMI supplemented with 10% fetal bovine serum, penicillin (100 U/ml), streptomycin (100 μg/ml), 2 mM glutamine, and 5×10^{-5} M 2-mercaptoethanol. KSHV infection of DMVEC was verified by DNA PCR for amplification of the KS330 *Bam*HI fragment of the ORF26 gene, and reverse transcription (RT)-PCR for the spliced mRNA from the ORF29 gene (85). DMVEC were used for experiments when >90% of cells expressed ORF73 (LANA). Typically, 2% of infected cells in such LANA-positive cultures expressed the early lytic protein ORF59/PF-8 (24) and <1% of PF-8-positive cells expressed the late lytic glycoprotein protein ORF K8.1A/B (26). Viral antigen expression was detected by immunofluorescent staining as previously described (71). Antibodies against viral proteins were a generous gift from Bala Chandran. Where specified, primary DMVEC (pDMVEC) were obtained from Clonetics (BioWhittaker, Walkersville, Md.) and maintained as described for immortalized DMVEC but without selection. pDMVEC were infected with a recombinant strain of KSHV that expresses green fluorescent protein (GFP) under the control of the elongation factor-1 promoter (GFP-KSHV). This virus was constructed and generously provided by Jeffry Vieira (Fred Hutchinson Cancer Research Center, Seattle, Wash.). Infection of GFP-positive cells was initially confirmed by simultaneous detection of ORF73 by immunofluorescent staining.

RNA isolation and fluorescent labeling. RNA was isolated approximately 4 weeks after initial infection when >90% of the cells were LANA positive and showed the spindle cell phenotype. The two infected cultures designated I-8 and I-9 were harvested simultaneously with a mock-infected control culture. RNA was isolated from T75 flasks containing approximately 5×10^6 cells using the RNeasy RNA isolation kit (QIAGEN Inc., Valencia, Calif.). After DNase treatment and another round of RNeasy purification, Cy-3 labeled cDNA was prepared as described previously (92, 97). Briefly, poly(A) RNA was selectively amplified by one round of T7-polymerase-based linear amplification. The resulting cRNA was converted into Cy-3-labeled cDNA by reverse transcriptase.

cDNA microarrays. Arrays were generated at the R. W. Johnson Pharmaceutical Research Institute as previously described (97). IMAGE Clones were obtained from commercial sources (Research Genetics, Huntsville, Ala.), and sequences were verified prior to PCR amplification. Arrays were printed onto silane-coated slides (Corning) using a Generation III microarray spotter (Molecular Dynamics) printer. Each clone was spotted twice on each slide at nonadjacent positions. Each slide was visually inspected prior to immobilization of the DNA by baking. Labeled samples were hybridized to the slides overnight at 42°C. Each sample was hybridized to two slides. Fluorescent signals were detected by a confocal scanner (Molecular Dynamics) and quantified using Autogene software (Biodiscovery, Los Angeles, Calif.). In addition, each slide was visually inspected for correct grid alignment, spot morphology, and signal consistency, and obviously bad spots were eliminated from further analysis. Raw data were scaled by calculating the ratio of the mean of the individual array to the mean of all arrays. Each intensity value was divided by this scaling factor. All data were $\log_2$ transformed. The mean intensity and coefficient of variation (CV) were determined for the four values obtained with each sample. Mean intensities with CV of >50% were excluded. Ratios were determined by comparing the mean intensity values of infected and noninfected samples. Background was set as the mean of the lowest 5% of signals. If both infected and noninfected signals were below this background threshold, changes were not considered significant. The complete data set can be viewed at http://www.ohsu.edu/vgti/fruehkshv.htm.

Real-time RT-PCR. RNA was isolated using an RNeasy Total RNA kit (QIAGEN, Inc.). RNA samples were treated with RNase-free DNase I to remove any residual genomic DNA contamination (Ambion, Austin, Tex.). Quantification of RNA was performed by a two-step method. First, cDNA was synthesized using superscript II (Invitrogen). Synthesized cDNA was diluted in H_2O to a final concentration of 2 ng per reaction mixture. Real-time PCR was performed on an ABI-PRISM 7700 Sequence Detection System (Applied Biosystems, Foster City, Calif.). To compared mock- and KSHV-infected samples, relative quantification was performed as outlined in ABI user bulletin 2 (Relative quantitation of gene expression: ABI PRISM 7700 sequence detection system: user bulletin 2: Rev B). Depending on the primer efficiency validation, the standard curve method or comparative cycle threshold (C_T) method was performed as outlined in user bulletin 2 (ABI). The comparative C_T method compares the different samples by analyzing the differences in the threshold cycles between samples after normalization to an endogenous reference gene. Different concentrations of RNA transcripts between treatments will produce different C_T values as the sample with more gene transcripts will amplify at a greater rate, producing an earlier threshold signal over background. The differences between samples during the exponential phase of PCR amplification were calculated by the following equation: $\Delta\Delta C_T = (C_T \text{ Target} - C_{TGAPDH})\text{infected} - (C_T \text{ Target} - C_{TGAPDH})\text{mock}$ and converted to *n*-fold change units by the equation $2^{-\Delta\Delta C_T}$. To generate standard curves, Universal Human Reference RNA (Stratagene, La Jolla, Calif.) was employed in a dilution scheme. If the target gene was not present in the Universal RNA sample, KSHV-infected DMVEC RNA was used to generate a relative standard curve. The samples were normalized to endogenous GAPDH. The following primers were generated using primer express v1.1 (ABI): Jun-D NM_005354 forward, 5′-AGTTCCTCTACCCCAAGGTGG-3′, and reverse, 5′-TGTGTAAATCCTCCAGGGCC-3′; UBE4A NM_0047880 forward 5′-TGGAGGAAAATGGGCACAAA-3′, and reverse, 5′-AGACTGGAGGCAGCATGGG-3′; neuritin NM_016588 forward, 5′-AGCGTATCTGGTGCAGGCC-3′, and reverse, 5′-AAAGCCCTTGAAGACCGCA-3′; CXADR NM_001338 forward, 5′-GCAGGGATAGATTTTGTTGGTGA-3′, and reverse, 5′-GGCTGGCCACCATTTTGA-3′; ARHGEF6_D25304 forward, 5′-ACCATCCACAGGAAATGGACTATTT-3′, and reverse, 5′-CTTTACTCTTCAGCTTCCAAACACG-3′; CD36 NM_000072 forward 5′-GGAAAATGTAACCCAGGACGC-3′, and reverse, 5′-GAAGGTTCGAAGATGGCACC-3′; IGFBP2 NM_000597 forward, 5′-CTGTGACAAGCATGGCCTGTA-3′, and reverse, 5′-TCACACACCAGCACTCCCC-3′; IGFBP6 NM_002178 forward, 5′-AGGGTCTCCAGATGGCAATG-3′, and reverse, 5′-CCCCTCTATCCCCCAGCTT-3′; INSR NM_000208 forward, 5′-GGGACCGCTTTACGCTTCTT-3′, and reverse, 5′-ACTCGTCCGGCACGTACAC-3′; PPARG NM_005037 forward, 5′-CAAACACATCACCCCCCTG-3′, and reverse, 5′-AAACTGGCAGCCCTGAAAGA-3′; Inhibitor of DNA binding 1 NM_002165 forward, 5′-GAACCGCAAGGTGAGCAAG-3′, and reverse, 5′-TCCAACTGAAGGTCCCTGATG-3′; LIM domain only 2 NM_005574 forward, 5′-GACGGTCTCTGCGCATCCT-3′, and reverse, 5′-TGTCTTTCACCCGCATTGTC-3′; c-Mer proto-oncogene forward, 5′-CTGCACACGGTTGGGTAGATT −3′, and reverse, 5′-AGCACAGGATCTGCGTTGC-3′; cytochrome P450 forward, 5′-TCCAGCTTTGTGCCTGTCAC-3′, and reverse, 5′-GGGAATGTGGTAGCCCAAGA-3′; c-Kit ligand NM_000899K forward, 5′-CCAAAAGACTACATGATAACCCTCAA-3′, and reverse, 5′-CATCTCGCTTATCCAACAATGACT-3′; monocyte chemoattractant protein-1 (MCP-1) forward 5′-GCCAAGGAGATCTGTGCTGAC-3′, and reverse, 5′-GGTTTGCTTGTCCAGGTGGT-3′; and c-Kit X06182 forward 5′-CGGATCAATTCTGTCGGCA-3′, and reverse, 5′-CATCGTCGTGCACAAGCAG.

Reagents. The 2-phenylaminopyrimidine derivative STI 571 (Gleevec) was developed and generously provided by Elisabeth Buchdunger (Novartis, Basel, Switzerland). Stock solutions of STI 571 were prepared at 10 mmol/liter by dissolving 5 mg of STI 571 in 1 ml of phosphate-buffered saline and used fresh or stored at −20°C. Working solutions were diluted in endothelial-SFM immediately prior to use.

Immunofluorescent staining. For detection of c-Kit protein, DMVEC monolayers were rinsed in phosphate-buffered saline containing 1% bovine serum albumin and 0.02% sodium azide (staining buffer) and stained with an anti-c-Kit monoclonal antibody (clone 57A5 [Ancell, Bayport, Minn.] or Clone Nu-cKit [Research Diagnostics, Flanders, N.J.]) followed by a goat anti-mouse fluorescently labeled secondary conjugate (Biosource International, Camarillo, Calif.). For mock- and KSHV-infected DMVEC, or DMVEC infected with a c-Kit recombinant adenovirus (described below), a FITC-labeled second conjugate was used. For pDMVEC infected with GFP-KSHV, a rhodamine conjugate was used to allow simultaneous visualization of GFP in infected cells. All antibodies were used at a 1:100 dilution in staining buffer and incubated with cell monolayers for 60 min at 37°C. Primary antibody was omitted from duplicate monolayers to control for nonspecific binding of secondary conjugate. Stained cells were fixed in 2% paraformaldehyde, mounted, and examined on a Nikon fluorescent microscope.

Proliferation assays. Proliferation of mock- and KSHV-infected DMVEC was quantified using a standard colorimetric assay based on bioreduction of the tetrazolium salt XTT(Roche, Molecular Biochemicals, Indianapolis, Ind.). DMVEC were plated in Primaria 96-well trays (Becton Dickinson) at 5×10^4 cells/well and cultured in endothelial-SFM containing 1% HS and lacking additional growth supplements (basal medium). Recombinant human stem cell factor (SCF) (Collaborative Biomedical Products, Bedford, Mass.) (20, 50, 100 and 200 ng/ml) or SCF (50 ng/ml) and STI 571 (0.01, 0.1, 1 and 10 μM) were added in fresh basal medium 24 h after plating as designated by the experimental protocol. XTT was added 48 h later according to the manufacturer's instructions. Absorbance (490 nm) was read after 4 to 6 h on a Dynatech MR5000 microplate reader. The Jurkat human T cell line (JJK subline) was provided by Dan Littman. Jurkat cells (5×10^4 cells/well) were plated in 96-well trays in RPMI containing 5% FBS in the presence or absence of 50U/ml IL-2 (Sigma) and STI 571 (0.01, 0.1, 1 and 10 μM) and proliferation was measured at 48 h as described above.

Transformation assays. To promote a transformed phenotype, KSHV-infected DMVEC were cultured postconfluency in 35-mm-diameter Primaria culture dishes. Under these conditions, cells assumed a pronounced spindle morphology, exhibited a disorganized growth pattern, and developed multilayered foci within the monolayer. Uninfected DMVEC cultured under similar conditions displayed growth inhibition and maintained a cobblestone phenotype with organized cell borders. Postconfluent cells were exposed to increasing doses of STI 571 (0.01, 0.1, 1, and 10 μM) that were replenished every 36 to 48 h using dilutions freshly prepared from a frozen stock. In other experiments, postconfluent cells were infected with a recombinant adenovirus expressing a dominant negative c-Kit protein (described below). DMVEC were examined daily for evidence of phenotypic change using a phase-contrast microscope and results recorded photographically.

Construction and use of adenovirus vectors. For overexpression of c-Kit in DMVEC in the absence of KSHV infection, full-length human c-Kit cDNA (65) was cloned into an adenoviral expression vector as previously described (101) to create a recombinant adenovirus expressing wild type c-Kit (Ad/c-KitWT). This places Ad/c-KitWT under the control of a *tet*-regulated promoter-enhancer element, and protein expression is driven by coinfection with an adenovirus expressing the requisite transactivator (Ad/trans). A dominant-negative c-Kit mutant (Ad/c-KitDN) was constructed by insertion of a premature stop codon at Ser_{614} in the cytoplasmic domain using standard PCR-based mutagenesis. Truncation of c-Kit at this site deletes the ATP-binding and phosphotransferase domains without affecting the dimerization domain. Following DNA sequence analysis to confirm correct mutagenesis, Ad/c-KitDN was similarly cloned into an adenoviral expression vector. Recombinant viruses were screened by PCR, and protein expression was confirmed by western immunoblot of infected cell lysates using a rabbit polyclonal antibody directed against the N terminus of c-Kit (H-300; Santa Cruz Biotechnology, Inc., Santa Cruz, Calif.). Recombinant adenoviruses were plaque purified, and viral stocks were grown and their titers were determined on 293 cells. For DMVEC infection, monolayers were incubated with Ad/c-KitWT or Ad/c-KitDN at a multiplicity of infection (MOI) of 10 and 100 and Ad/trans at an MOI of 10 for 4 h at 37°C. Optimal MOI doses were previously determined, and virus stocks were diluted in medium containing 2% human serum and Polybrene (4 μg/ml; Sigma) for infection. As a control for infection efficiency and nonspecific effect of adenovirus infection, duplicate monolayers were infected with an adenovirus vector expressing green fluorescent protein (Ad/GFP). Infection with Ad/GFP and Ad/trans at MOI of 100 and 10, respectively, allowed infection of >80% of cells in culture with minimal cytopathic effect.

RESULTS

DNA-microarray analysis of KSHV-infected DMVEC. DMVEC cultures immortalized with HPV-E6/E7 (DMVEC) were either mock infected or infected with two different stocks of KSHV derived from the BCBL-1 PEL cell line as previously described (71). Each infected culture was propagated separately for approximately 4 weeks until >90% of cells were latently infected, as determined by spindle morphology and expression of LANA (data not shown). Mock-infected cells were grown and harvested in parallel. Total RNA was isolated, labeled with Cy-3, and hybridized to cDNA arrays displaying a

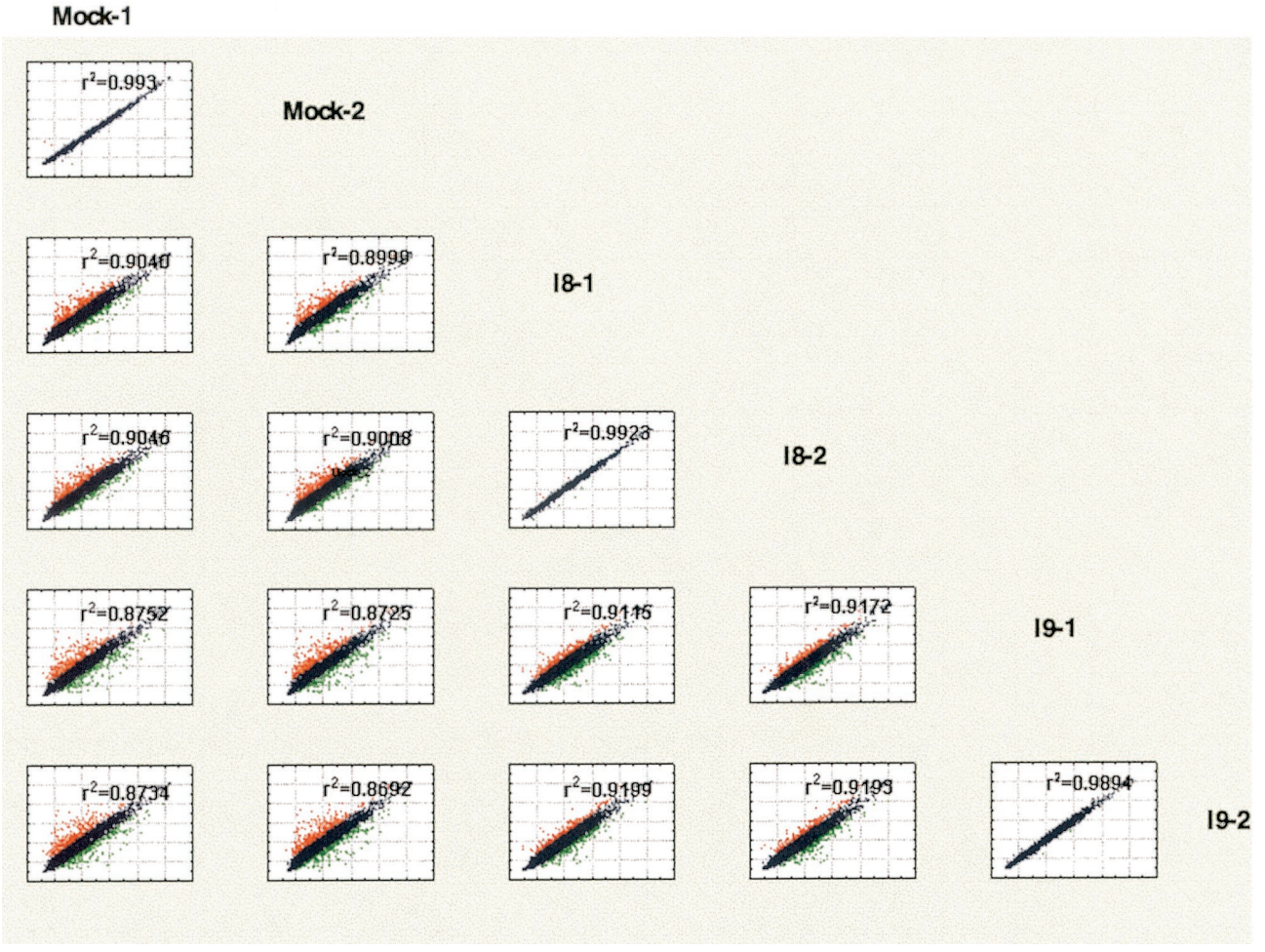

FIG. 1. Comparison matrix of normalized intensity values from microarray slides by scatter plot. Normalized logarithmic intensity values obtained from each individual array were compared between each sample and depicted as a scatter plot. The annotation of the *x* axis is shown to the right of the matrix, whereas the *y* axis annotation is shown on top. Values that differ more than 1.8-fold are shown in red (high) or green (low). Also shown is the correlation coefficient r^2 for each comparison. The highest correlation was observed when for results obtained from the same sample hybridized to two arrays. Comparisons between the two different infected samples, I-8 versus I-9, were more similar to each other than comparisons between infected samples and mock-infected DMVEC isolated in parallel.

total of 4,165 clones in duplicate. Each RNA sample was hybridized to two arrays. Comparison of the signal intensities between the two arrays probed for each sample revealed a low interarray variation (Fig. 1). When the expression profiles of the two infected cell lines (designated I-8 and I-9) were compared to each other and to the mock-infected culture, the infected cultures were more closely correlated to each other than to the mock-infected cells (Fig. 1). However, differences in expression profiles between the two infected cultures also became apparent. To account for this experimental variation, we considered only genes that were up- or downregulated ≥1.8-fold in both infected cell lines compared to the mock-infected cell line. These ratios were calculated using the mean of the intensities of both replicate chips, i.e., a total of four measurements per gene for each of the three samples. Only those results with a CV of <50% were included. Approximately 45% of the clones that changed more than twofold in one of the infected cell cultures, also changed significantly in the other experiment resulting in 184 clones changing significantly in both experiments. The ratios for these differentially expressed genes are shown in Table 1. If several clones represented the same gene, results for all individual clones are shown. The complete data set can be viewed at http://www.ohsu.edu/vgti/fruehkshv.htm.

To confirm the cDNA array results by an independent method, real-time RT-PCR analysis on mock- and KSHV-infected samples was carried out for 16 selected genes. In addition to the RNA samples used for the array analysis, we also determined the RNA expression levels for these genes in two additional independently derived KSHV cultures in comparison to a parallel culture of mock-infected cells. Specific primers were selected based on the UniGene sequence containing the respective accession number. Relative quantification of gene expression in mock- and KSHV-infected samples was performed as described in the Materials and Methods section. The ratios determined in comparison to mock-infected samples are shown in Table 2. The majority of the genes tested showed a higher induction or repression ratio when analyzed

TABLE 1. Genes modulated in DMVEC after KSHV infection[b]

UG Cluster	Gene ID	Symbol	cDNA array value for:		Name	Function	Group[a]
			I8	I9			
Hs.75613	N39161	CD36	14.9	27.0	CD36 (thrombospondin receptor)	Platelet-collagen adhesion	A
Hs.110802	AA487787	VWF	4.6	9.3	von Willebrand factor	Antihemophilic factor carrier	A
Hs.12337	AA026831	KDR	3.9	4.3	VEGF receptor 2	Vascular development, angiogenesis	A
Hs.75716	T49159	SERPINB2	2.3	2.9	Plasminogen activator inhibitor 2	Angiogenesis	A
Hs.295944	L27624	TFPI2	**−2.1**	**−3.5**	Tissue factor pathway inhibitor 2	Inhibit trypsin, factor VII(a)/tissue factor	A
Hs.1908	AA278759	PRG1	**−2.1**	**−9.3**	Proteoglycan 1, secretory granule	Tissue development and maintenance	A
Hs.77274	AA284668	PLAU	**−2.8**	**−10.6**	Urokinase plasminogen activator	Angiogenesis	A
Hs.8966	H58644	TEM8	**−5.0**	**−16.7**	Anthrax toxin receptor	Elevated during tumor angiogenesis	A
Hs.78146	R22412	PECAM1	2.7	1.8	CD31	Expressed on cell intercellular junctions	A
Hs.268107	AA423867	MMRN	9.3	5.0	Endothelial cell multimerin precursor	Extracellular matrix, adhesion	CA
Hs.81337	AA434102	LGALS9	3.3	2.4	Lectin, galactoside binding	Cell adhesion	CA
Hs.50964	AA411757	CEACAM1	2.7	3.5	CD66 antigen	Cell adhesion	CA
Hs.2340	R06417	JUP	2.0	2.4	Junction plakoglobin	Cell adhesion	CA
Hs.118787	R31321	TGFBI	**−2.6**	**−2.9**	Transforming growth factor	Inhibits cell adhesion	CA
Hs.36131	AA167222	COL14A1	**−3.3**	**−3.5**	Collagen, type XIV, alpha 1	Interacts with type I collagen	CA
Hs.179573	AA490172	COL1A2	**−4.5**	**−10.1**	Collagen, type I, alpha 2	Fibrillar forming collagen	CA
Hs.156346	AA504348	TOP2A	4.3	4.7	Topoisomerase (DNA) II alpha	DNA synthesis	CD
Hs.69563	H59203	CDC6	3.7	2.6	CDC6 homolog	Cell growth and differentiation	CD
Hs.239	AA129552	FOXM1	3.5	3.5	Forkhead box M1	Cell proliferation	CD
Hs.85137	AA608568	CCNA2	3.4	2.6	Cyclin A2	Regulators of CDK kinases	CD
Hs.156346	AA504348	TOP2A	3.2	3.2	Topoisomerase (DNA) II alpha	DNA replication	CD
Hs.84113	AA284072	CDKN3	2.8	2.9	Cyclin-dependent kinase inhibitor 3	Cell growth and differentiation	CD
Hs.166563	H73714	RFC1	2.6	2.3	Replication factor C (activator 1) 1	Activator of DNA polymerases	CD
Hs.348669	AA459292	CKS1	2.6	2.2	CDC28 protein kinase 1	Cell growth and differentiation	CD
Hs.79069	AA489752	CCNG2	2.4	1.8	Cyclin G2	Regulators of CDK kinases	CD
Hs.75586	H84153	CCND2	2.2	2.7	Cyclin D2	Regulators of CDK kinases	CD
Hs.179565	AA455786	MCM3	2.2	2.2	DNA replication licensing factor mcm3	Associates with DNA polymerase	CD
Hs.78996	AA450265	PCNA	2.0	2.1	Proliferating cell nuclear antigen	Cell growth and differentiation	CD
Hs.115474	H94617	RFC3	1.9	1.9	Replication factor C (activator 1) 3	DNA strand elongation	CD
Hs.154762	W52273	HRB2	**−1.9**	**−3.8**	HIV-1 rev binding protein 2	May be required for cell division	CD
Hs.256290	AA464731	S100A11	**−2.0**	**−3.7**	S100 calcium binding protein A11	Cell cycle progression, differentiation	CD
Hs.514	AA454146	CCNH	**−2.4**	**−2.0**	Cyclin H	Regulators of CDK kinases	CD
Hs.103291	R66101	LOC51299	5.0	7.7	Neuritin	Neurite outgrowth	CS
Hs.296842	AA490477		4.0	6.4	Similar to nonmuscle myosin	Cytokinesis and cell shape	CS
Hs.79226	H20758	FEZ1	3.8	3.5	Zeta 1	Axonal outgrowth	CS
Hs.195850	AA160507	KRT5	2.3	2.4	Keratin 5	Intermediate filament family	CS
Hs.79307	AA236617	ARHGEF6	2.2	3.1	Rac/Cdc42 guanine exchange factor 6	Regulation of actin cytoskeleton	CS
Hs.121576	W95682	MYO1B	2.0	3.1	Myosin IB	Cytoskeleton	CS
Hs.182265	AA464250	KRT19	1.8	1.8	Keratin 19	Cytoskeletal structural protein	CS
Hs.160483	R62868	EPB72	1.8	2.4	Erythrocyte membrane protein	Cytoskeleton	CS
Hs.24178	R27680	EML2	**−1.9**	**−2.5**	Microtubule-associated protein-like protein 2	Assembly dynamics of microtubules	CS
Hs.155524	T64878	PNUTL2	**−1.9**	**−2.0**	Peanut-like 2 (*Drosophila*)	Cytoskeletal organization	CS
Hs.12451	AA447196	EML1	**−3.7**	**−7.1**	Microtubule-associated protein-like protein 1	Assembly dynamics of microtubules	CS
Hs.303649	AA425102	SCYA2	7.0	9.2	Monocyte chemotactic protein-1	Inflammation	H
Hs.20144	R96668	SCYA14	5.5	38.9	CC-chemokine 14	Inflammation	H
Hs.182579	R69307	LOC51056	5.1	2.2	Leucine aminopeptidase	Interferon gamma induced	H
Hs.83429	H54629	TNFSF10	4.2	3.8	Tumor necrosis factor superfamily	Induces apoptosis	H
Hs.82112	AA464525	IL1R1	3.8	7.8	Interleukin 1 receptor, type I	Cell signalling	H
Hs.285401	AA279147	CSF2RB	3.3	2.1	Colony-stimulating factor 2 receptor	High-affinity receptor for IL-3, IL-5, CSF	H
Hs.44532	N49629	UBD	2.0	2.8	Diubiquitin	Gamma interferon induced	H
Hs.237356	AA447115	SDF1	**−2.0**	**−2.3**	Stromal cell-derived factor 1	Chemokine	H
Hs.12013	T70122	ABCE1	2.4	1.8	ATP-binding cassette	Antipathogen response	H
Hs.1869	AA488504	PGM1	5.3	3.3	Phosphoglucomutase 1	Breakdown and synthesis of glucose	M
Hs.154654	AA448157	CYP1B1	5.1	10.9	Cytochrome P450, subfamily I	Drug metabolims and lipid biosynthesis	M
Hs.84190	R49999	SLC19A1	4.3	6.6	Solute carrier family 19, member 1	Folate transport	M
Hs.76057	AA281030	GALE	2.5	2.5	Galactose-4-epimerase, UDP^{-}	Galactose metabolism	M
Hs.268012	W31074	FACL3	2.5	2.1	Fatty-acid-coenzyme A ligase	Lipid synthesis and fatty acid degradation	M
Hs.59403	AA160852	SPTLC2	2.4	2.2	Serine palmitoyltransferase	Sphingolipids	M
Hs.183556	T70098	SLC1A5	2.2	2.5	Solute carrier family 1, member 5	Neutral amino acid transporter	M
Hs.75694	AA482198	MPI	2.1	2.7	Mannose phosphate isomerase	Mannosylation	M
Hs.183868	N34827	GUSB	1.9	3.5	Glucuronidase, beta	Degradation of dermatan sulfates	M
Hs.75736	H15842	APOD	1.8	10.5	Apolipoprotein D	Lipoprotein metabolism	M
Hs.251415	N74025	DIO1	**−1.8**	**−6.2**	Deiodinase, iodothyronine, type I	Oxidoreductase	M
Hs.73875	H44956	FAH	**−2.0**	**−2.0**	Fumarylacetoacetate hydrolase	Fumarylacetoacetase	M
Hs.234642	R91904	AQP3	**−2.2**	**−2.3**	Aquaporin 3	Small molecule transport	M
Hs.306098	R93124	AKR1C1	**−2.3**	**−2.8**	Dihydrodiol dehydrogenase	Metabolizes xenobiotics	M

Continued on following page

TABLE 1—*Continued*

UG Cluster	Gene ID	Symbol	DNA array value for:		Name	Function	Group[a]
			I8	I9			
Hs.81454	T61308	KHK	1.8	2.0	Ketohexokinase (fructokinase)	Transferase	M
Hs.576	N95761	FUCA1	1.9	1.8	Fucosidase, alpha-L-1, tissue	Glycosyl hydrolases	M
Hs.79187	N31467	CXADR	7.2	8.6	Coxsackie virus/adenovirus receptor	Pathogenic invasion	O
Hs.75737	AA164439	PCM1	3.9	3.3	Perioentriolar material 1	Interacts with centrosome	O
Hs.3314	AA070226	SEPP1	3.5	3.5	Selenoprotein P, plasma, 1	Oxidative stress response	O
Hs.284186	AA495846		3.2	3.3	Transcription factor forkhead-like 7	Binding of freac-3 and freac-4	O
Hs.74471	AA487623	GJA1	2.3	2.2	Gap junction protein, alpha 1	Cell-to-cell communication	O
Hs.153487	AA485996	STAM	**−1.8**	**−2.0**	Signal transducing adaptor molecule 1	Signal transduction	O
Hs.234680	H26176	FER1L3	**−2.1**	**−3.8**	Myoferlin (for-1 like protein 3)	Role in membrane regeneration	O
Hs.13046	AA453335	TXNRD1	**−2.1**	**−3.9**	Thioredoxin reductase 1	Thioredoxin reductase (NADPH)	O
Hs.36927	AA485036	HSP105B	**−2.1**	**−1.8**	Heat shock 105kD	Heat shock response	O
Hs.75510	AA465051	ANXA11	**−2.6**	**−2.3**	Annexin A11	Phospholipid-binding protein	O
Hs.56023	AA262988	BDNF	**−2.7**	**−5.4**	Brain-derived neurotrophic factor	Neural growth factor	O
Hs.89137	AA464566	LRP1	**−2.7**	**−3.3**	Low-density lipoprotein-related protein	Binds to apoE-containing lipoproteins	O
Hs.296323	H75599	SGK	**−2.7**	**−3.2**	Serum/glucocorticoid-regulated kinase	Stress response	O
Hs.135084	AA599177	CST3	**−3.4**	**−2.1**	Cystatin C	Inhibitor of cysteine proteinases	O
Hs.8265	R97066	TGM2	**−3.6**	**−4.5**	Transglutaminase 2	Protein modification	O
Hs.790	AA495936	MGST1	**−6.6**	**−9.4**	Microsomal glutathione *S*-transferase	Conjugation of reduced glutathione	O
Hs.93002	AA430504	UBE2C	4.3	3.5	Ubiquitin-conjugating enzyme E2C	Ubiquitination	PD
Hs.155485	H78483	HIP2	3.3	2.0	Ubiquitin-conjugating enzyme e2–25	Huntington interacting protein 2	PD
Hs.75275	AA447528	UBE4A	2.2	3.5	Ubiquitination factor E4A	Ubiquitination	PD
Hs.1565	AA442095	NEDD4	**−1.9**	**−9.0**	NEDD-4	Ubiquitination	PD
Hs.84084	AA046411	APPBP2	6.8	3.6	Amyloid beta precursor protein	Vesicie sorting	PS
Hs.20830	N69491	KNSL2	2.4	2.3	Kinesin-like 2	Microtubule gliding	PS
Hs.1050	AA480859	PSCD1	2.4	2.5	Pleckstrin homology	Protein sorting, membrane trafficking	PS
Hs.91728	AA458994	PMSCL1	3.2	2.2	Polymyositis/scleroderma autoantigen	3 processing of the 7s pre-MA	PT
Hs.79306	AA193254	EIF4E	3.0	1.8	Eukaryotic translation initiation factor	Transcription factor	T
Hs.78995	AA234897	MEF2C	2.7	2.4	MADS box transcription	Transcriptional activator	T
Hs.54452	AA280931	ZNFN1A1	2.4	2.2	Zinc finger protein, subfamily 1A	Transcriptional activator	T
Hs.33287	W87611	NFIB	2.2	2.9	Nuclear factor I/B	Transcription regulation	T
Hs.81328	W55872	NFKBIA	2.2	1.8	NF-KAPPAB INHIBITOR ALPHA	Transcription factor	T
Hs.181163	H93087	HMG17	2.1	1.8	High-mobility group protein 17	Bind to nucleosomal DNA	T
Hs.154095	AA443659	ZNF143	2.0	3.9	Zinc finger protein 143	Transcriptional activator	T
Hs.79353	W33012	TFDP1	2.0	2.1	Transcription factor Dp-1	Transcription regulation	T
Hs.7943	R63137	RMP	**−2.1**	**−2.3**	RPB5-mediating protein	Transcription regulation from Pol II	T
Hs.159223	AA434487	NAB2	**−2.2**	**−2.1**	NGFI-A binding protein 2	Transcriptional corepressor	T
Hs.89657	AA292583	TAF10	**−2.4**	**−1.8**	TAF10 RNA polymerase II	TFIID complex	T
Hs.159223	AA434487	NAB2	**−2.4**	**−2.4**	NGFI-A binding protein 2	Transcriptional repressor	T
Hs.2780	AA418670	JUND	5.2	7.8	*jun*-D proto-oncogene	Transcription regulation	TG
Hs.100724	AA088517	PPARG	4.3	6.0	PPAR gamma	Adipocyte differentiation	TG
Hs.75424	AA457158	ID1	4.0	6.1	Inhibitor of DNA binding 1	Transcription regulation	TG
Hs.184585	AA464644	LMO2	3.5	7.8	LIM domain only 2 (rhombotin-like 1)	Hematopoietic development	TG
Hs.179718	AA456878	MYBL2	3.3	6.1	Myb-related protein b (b-myb)	Oncogenesis	TG
Hs.2969	W69471	SKI	3.0	5.9	*ski* oncogene	Oncogenesis	TG
Hs.22026	R16604		2.9	3.8	Similar to transmembrane 4	Expressed in endothelial cells and tumors	TG
Hs.10526	T59334	CSRP2	2.7	2.3	Cysteine-and glycine-rich protein 2	Development and cellular differentiation	TG
Hs.81665	N20798	KIT	2.6	5.0	c-*kit*	Hematopoietic development	TG
Hs.117078	AA436591		2.6	2.9	Cellular proto-oncogene (c-mer)	Oncogenesis	TG
Hs.31137	T69540	PTPRE	2.4	2.6	Protein tyrosine phosphatase	Oncogenesis	TG
Hs.89695	AA001614	INSR	2.1	3.4	Insulin receptor	Cell growth and maintenance	TG
Hs.162	H79047	IGFBP2	2.1	3.9	IGF binding	Cell growth and differentiation	TG
Hs.1103	R36467	TGFB1	2.1	2.4	Transforming growth factor, beta 1	Proliferation, differentiation, apoptosis	TG
Hs.25155	R24543	NET1	1.9	2.7	Neuroepithelial cell transforming gene	Oncogenesis	TG
Hs.194143	H90415	BRCA1	1.9	2.2	Breast cancer 1, BRCA 1	Transcriptional activator	TG
Hs.326035	AA486628	EGR1	1.8	2.2	Early growth response 1	Transcriptional regulator	TG
Hs.61796	AA399334	TFAP2C	**−1.8**	**−2.1**	Transcription factor AP-2 gamma	Oncogenesis	TG
Hs.129914	AA425238	RUNX1	**−2.0**	**−1.4**	Runt-related transcription factor	Oncogenesis	TG
Hs.75551	AA235332	RSU1	**−2.2**	**−1.8**	Ras suppressor protein 1	Inhibits Ras signaling	TG
Hs.279860	R09634	TPT1	**−2.6**	**−2.1**	Tumor protein	Unknown	TG
Hs.1298	R98851	MME	**−5.4**	**−8.1**	Membrane metallo-endopeptidase	Marker of acute lymphocytic leukemia	TG
Hs.23582	AA454810	TACSTD2	**−5.4**	**−2.3**	Transducer 2	Growth factor receptors	TG
Hs.274313	AA478724	IGFBP6	**−1.9**	**−4.7**	Insulin-like growth factor binding	Cell growth inhibitor	TG
Hs.325823	H69048		6.6	16.8	Similar to ZN91	Unknown	U
Hs.325823	R63109		4.9	8.0	Novel	Unknown	U
Hs.170234	R69677		4.7	14.0	Novel	Unknown	U
Hs.38516	W02617		4.6	12.0	Similar to developmental protein	Unknown	U
Hs.8769	N57594	BCMP1	3.9	4.2	Brain cell membrane protein 1	Homology to Wikott-Aldrich syndrome	U

Continued on facing page

TABLE 1—*Continued*

UG Cluster	Gene ID	Symbol	DNA array value for:		Name	Function	Group[a]
			I8	I9			
Hs.23044	W00895	MGC16386	3.5	3.1	Novel	Unknown	U
Hs.107528	T67558	AIG-1	3.5	3.4	Androgen-induced protein	Unknown	U
Hs.111577	AA034213	ITM3	3.5	6.3	Integral membrane protein 3	Unknown	U
Hs.51615	T70413		3.2	4.7	Novel	Unknown	U
Hs.16951	R91083		2.9	3.8	DKFZP586P2219	Unknown	U
Hs.16951	T85698		2.9	3.5	Novel	Unknown	U
Hs.28456	R63982		2.9	3.4	Novel	Unknown	U
Hs.28456	H80158		2.9	8.9	Novel	Unknown	U
Hs.107528	R01796	AIG-1	2.7	3.2	Androgen-induced protein	Unknown	U
Hs.28783	R23302	KIAA1223	2.7	2.1	KIAA1223 protein	Unknown	U
Hs.20558	R70925	FLJ20345	2.6	2.1	Novel	Unknown	U
Hs.104859	T66936		2.5	2.8	DKFZp762E1312	Unknown	U
Hs.151334	H65042		2.5	3.9	Novel	Unknown	U
Hs.326416	N55339		2.5	3.0	Novel	Unknown	U
Hs.191558	R06370		2.4	3.4	Novel	Unknown	U
Hs.191558	N91307		2.3	2.7	Novel	Unknown	U
Hs.191558	R79935		2.2	2.0	Novel	Unknown	U
Hs.26516	N72697	FLJ10604	2.1	4.6	Novel	Unknown	U
Hs.13041	T67104		2.1	2.8	Novel	Unknown	U
Hs.13041	AA452909		2.1	3.6	Novel	Unknown	U
Hs.13041	AA430744		2.1	2.0	Novel	Unknown	U
Hs.13041	R28344		2.0	2.3	Novel	Unknown	U
Hs.180059	N67039		1.9	1.8	Novel	Unknown	U
Hs.19717	R11532		1.9	2.2	Novel	Unknown	U
Hs.64313	T66828		1.8	2.3	Novel	Unknown	U
Hs.122546	H83176	FLJ23017	1.8	3.2	Novel	Unknown	U
Hs.20654	R10682		1.8	2.3	Novel	Unknown	U
Hs.38163	H63202		1.8	6.1	Hypothetical protein	Unknown	U
Hs.38163	R06507		1.8	1.9	Novel	Unknown	U
Hs.38163	AA452909		1.8	3.3	Novel	Unknown	U
Hs.23016	N53172	RDC1	1.8	4.6	RDC1 G protein-coupled receptor	Unknown	U
Hs.18878	R00332	EGLN3	1.8	2.2	EGL nine homolog 3	Unknown	U
Hs.6349	AA432023	BC008967	**−1.8**	**−2.6**	Novel	Unknown	U
Hs.37308	H56438		**−1.8**	**−1.9**	Novel	Unknown	U
Hs.187447	T97870		**−1.8**	**−2.4**	Novel	Unknown	U
Hs.37623	H58834		**−1.8**	**−1.9**	Novel	Unknown	U
Hs.79123	AA457047	KIAA0084	**−1.9**	**−2.7**	Novel	Unknown	U
Hs.297929	R67991		**−1.9**	**−5.6**	Novel	Unknown	U
Hs.20588	H66312	PPY2	**−2.0**	**−2.1**	Pancreatic polypeptide 2	Unknown	U
Hs.165067	H53316		**−2.0**	**−3.3**	Novel	Unknown	U
Hs.170198	AA459109	KIAA0009	**−2.0**	**−3.2**	Novel	Unknown	U
Hs.170198	N91330		**−2.0**	**−2.7**	Novel	Unknown	U
Hs.82141	H64850		**−2.0**	**−2.5**	Novel	Unknown	U
Hs.271686	R87194		**−2.1**	**−3.1**	Novel	Unknown	U
Hs.351310	N69540		**−2.2**	**−1.8**	Novel	Unknown	U
Hs.285519	AA447098		**−2.2**	**−3.4**	Novel	Unknown	U
Hs.285519	AA455538		**−2.3**	**−6.2**	Novel	Unknown	U
Hs.35453	R95811		**−2.7**	**−3.5**	cDNA DKFZp761G151	Unknown	U
Hs.78019	H79234		**−2.9**	**−2.6**	Novel	Unknown	U
Hs.78019	AA284568		**−3.3**	**−3.6**	Novel	Unknown	U

[a] Genes are organized into the following groups: A, angiogenesis; CA, cell adhesion; CD, cell division; CS, cell shape; H, host defense; M, metabolism; O, other; PD, protein degradation; PS, protein sorting; PT, protein translation; T, transcription; TG, tumorigenesis; U, unknown.
[b] Boldface type indicates down regulated genes.

by real-time PCR compared to the array results. This may reflect the wider dynamic range of quantitative real-time PCR compared to cDNA array detection systems and is commonly observed when comparing cDNA array data and real-time PCR (80, 115). Importantly however, RT-PCR confirmed the induction or repression detected by cDNA array for the majority of the genes, both in the two KSHV-infected samples used for array analysis and in the two independently derived infected cultures.

A functional description of the differentially expressed genes is shown in Table 1, and where possible, gene products are grouped into functional classes. Thirty-six of the clones that scored as upregulated genes in the cDNA array experiment, and 17 of the down-regulated clones, harbored sequences with unknown function. The remaining gene products were classified according to known functions in tumorigenesis, angiogenesis, host defense, cell adhesion, cell shape, cell division, transcription, metabolic pathways, or various other functions. With

TABLE 2. Real-time PCR confirmation of cDNA data

UG Cluster	cDNA array value for:		Quantitative RT-PCR result for:				Name
	I8	I9	I8	I9	B1	B2	
Hs.75613	14.9	27.0	159.5	681.8	1.9	4.1	CD36 (collagen type I receptor, thrombospondin receptor)
Hs.103291	5.0	7.7	7.0	40.5	2.8	3.0	Neuritin
Hs.79307	2.2	3.1	9.2	23.6	2.8	2.1	Rac/Cdc42 guanine exchange factor (GEF) 6
Hs.303649	7.0	9.2	6.5	8.5	8.1	8.2	MCP-1
Hs.154654	5.1	10.9	41.5	30.1	10.1	14.7	Cytochrome P450, subfamily 1
Hs.79187	7.2	8.6	9.5	20.0	4.0	4.9	Coxsackie virus and adenovirus receptor
Hs.75275	2.2	3.5	1.3	1.1	−2.0	−1.3	Ubiquitination factor E4A (homologous to yeast UFD2)
Hs.2780	5.2	7.8	1.8	4.0	3.2	2.8	*jun*-D proto-oncogene
Hs.100724	4.3	6.0	8.7	1.7	6.0	3.1	Peroxisome proliferative activated receptor, gamma
Hs.75424	4.0	6.1	5.8	2.6	1.7	1.4	Inhibitor of DNA binding 1
Hs.184585	3.5	7.8	13.0	53.7	4.2	2.7	LIM domain only 2 (rhombotin-like 1)
Hs.81665	2.6	5.0	23.6	44.5	157.6	89.0	c-*kit*
Hs.117078	2.6	2.9	12.1	19.2	5.0	4.5	Human cellular proto-oncogene (c-mer)
Hs.89695	2.1	3.4	5.1	8.6	10.3	10.7	Insulin receptor
Hs.162	2.1	3.9	13.3	29.5	8.5	8.4	Insulin-like growth factor binding protein 2 (36 kDa)
Hs.274313	−1.9	−4.7	−1.9	−4.8	−27.5	−35.2	Insulin-like growth factor binding protein 6

particular focus on those sequences that were confirmed by real-time PCR, we will discuss some of these gene products with respect to their potential involvement in KS.

Host defense genes. Several of the KSHV-induced genes belonged to the interferon or proinflammatory pathways. Induction of interferon-regulated genes and pro-inflammatory genes is likely to reflect host cell defense mechanisms against KSHV infection and is often observed in virally infected cells (43). However, in contrast to what is seen with acute human cytomegalovirus infection (97), we did not detect a massive induction of the interferon-response genes in these experiments. The upregulation of the pro-inflammatory chemokine MCP-1 was confirmed by real-time PCR. MCP-1 (or CCL2) is a CC-chemokine that attracts mononuclear cells to sites of inflammation (72). Consistent with our observation, strong MCP-1 expression has also been noted in KS-derived spindle cells (94). The CC-chemokine 14 was also induced in our experiments. A potential role for this chemokine in inflammation is inferred from homology, but has not been demonstrated experimentally (77). One of the hallmarks of KS lesions is their abundant infiltration by macrophages, lymphoid cells, mast cells, and neutrophils (37). It is likely that KSHV-induced host genes such as MCP-1, in combination with viral genes such as vMIPs, contribute to this inflammatory process in vivo.

Cell adhesion and cell shape. Infection of endothelial cells with KSHV generates a spindle cell morphology and induces focus formation (31, 60, 71). These phenotypic changes were reflected in the observed induction of genes regulating cell shape. The induction of two transcripts, neuritin and CDC42/Rac, was confirmed by real-time PCR. Neuritin has been shown to promote neurite outgrowth and arborization in primary neuronal cultures (74) and could thus be involved in the morphological changes seen in KSHV-infected DMVEC. CDC42/Rac is a major link between signaling pathways and the regulation of actin cytoskeleton rearrangements. Since CDC42 is involved in cell growth and differentiation (38), it may play a role in the morphological transformation of endothelial cells following KSHV infection.

Angiogenesis. KS lesions are characterized by extensive neoangiogenesis (37). This is reflected in our endothelial cell system by vessel-like aggregates of KSHV-infected spindle cells in cultures maintained for prolonged periods of time (data not shown). Vascular endothelial growth factor (VEGF) plays a key role in angiogenic processes, and VEGF has been shown to be induced by virally encoded gene products including vIL-6, vGCR, vMIP-I, and vMIP-II (5, 9, 64, 98). Therefore, it is notable that the type 2 receptor for VEGF (VEGF-R2/KDR) was upregulated in our experiment since it suggests the possibility of an autocrine proangiogenic and proliferative stimulation. Upregulation of VEGF-R2 on KSHV-infected endothelial cells has been shown by others (42) and was confirmed on our KSHV-infected DMVEC by immunofluorescent staining (data not shown). Another upregulated gene confirmed by real time PCR in our system was that for the endothelial cell marker CD36, which is also expressed on KS spindle cells in vivo (89). CD36 is a multiligand scavenger receptor that binds to thrombospondin-1, collagen, oxidized low density lipoproteins, and long-chain fatty acids (40). Since thrombospondin is a potent inhibitor of angiogenesis (105), the high level of CD36 induction in KSHV-infected cells could thus suggest a therapeutic mechanism to counteract KSHV-induced proangiogenic factors such as VEGF with exogenous thrombospondin.

Another important step in angiogenesis is extracellular matrix degradation and remodeling (for a recent review, see reference 79). The fibrinolytic plasminogen/plasmin system degrades most ECM-components. Plasminogen activator (uPA) cleaves plasminogen into plasmin, the active protease. Interestingly, the inhibitor of plasminogen activator was induced in KSHV-transformed DMVEC, whereas expression of uPA was repressed. This suggests that ECM degradation does not occur via plasminogen activation from KSHV-infected cells.

Cell division. A number of genes that play a role during the cell cycle and DNA replication were upregulated in KSHV-infected cells. The KSHV-encoded viral cyclin, vCYC/ORF72, expressed in all latently infected cells, might play a role in these changes in cell cycle regulation (23, 104).

Tumorigenesis. Carcinogenesis is often the result of aberrant cellular differentiation. Peroxisome proliferator-activated receptor gamma (PPAR-γ) is a ligand-activated nuclear receptor regulating adipocyte differentiation and carcinogenesis (39). PPAR-γ upregulation identified by microarray analysis was confirmed in real-time PCR experiments. The upregulation of PPAR-γ could be responsible for the regulation of several genes in our experiments since it has been shown that PPAR-γ agonists induce CD36 (108), plasminogen-activator inhibitor (55), and several genes regulating fatty-acid metabolism (39). In turn, PPAR-γ expression is upregulated by insulin and insulin-like growth factor 1 (IGF-1) (87). IGFs are known inducers of endothelial cell differentiation and angiogenesis (10) and IGF-insulin receptor interactions have been implicated in various tumorigenic processes (6). Insulin-like growth factor binding proteins (IGFBPs) bind to IGFs, modulating their interactions with insulin receptors (46). Increased IGFBP-2 levels have been associated with tumorigenesis (54), while IGFBP-6 is antitumorigenic. In this context, it is interesting that both the insulin receptor and IGFBP-2 were induced in KSHV infected DMVEC, while IGFBP-6 was downregulated, as observed both by microarray and PCR analysis. The IGF-pathway might thus be central to the transformation of endothelial cells by KSHV.

We also confirmed the induction of several additional genes with known functions in tumor development: c-*kit*, *jun*-D, and c-*mer* and the genes coding for inhibitor of DNA binding 1 (ID1) and LIM domain protein (LMO2). Jun-D belongs to the c-Jun family of DNA binding proteins. It is activated by several signaling cascades such as the extracellular signal-regulated kinase and mitogen-activated protein kinase pathways and in turn activates a number of genes. ID family proteins are helix-loop-helix DNA binding proteins whose overexpression is associated with proliferation and arrested differentiation in many cell lineages. c-*mer* is normally expressed during embryonic development and in the monocytic lineage but is aberrantly expressed in neoplastic T- and B-cell lines (45). In macrophages, c-Mer is thought to regulate uptake of apoptotic cells (95). The proto-oncogene LMO2 encodes a LIM domain transcription regulator that controls angiogenesis during mouse embryogenesis by regulating remodeling of the capillary network into mature vessels (112). The LMO2 gene is activated by chromosomal translocations in human T cell acute leukemias (81). The differential regulation of genes known to be involved in tumor formation following infection of DMVEC is consistent with the transforming potential of KSHV.

KSHV induces the surface expression of c-Kit. The cDNA array analysis suggested many potentially important host-cell pathways that are modulated by KSHV during the transformation. We reasoned that some of these cellular genes would be crucial for KSHV-induced transformation. One of the genes that seemed a strong candidate for a pivotal role in endothelial cell transformation was the proto-oncogene c-*kit*. The c-Kit protein is a receptor tyrosine kinase for the ligand SCF, also known as steel factor or mast cell growth factor (67, 114). c-Kit induction by KSHV was of particular interest because c-Kit expression has been directly implicated in tumor etiology, due to activating mutations that allow ligand-independent activation, or coexpression of receptor and ligand leading to autocrine growth stimulation (12). c-Kit is normally expressed on hematopoietic cells, melanocytes, and germ cells but has also been detected in a variety of hematologic malignancies and solid tumors (63). Moreover, a recent study has also reported expression of c-Kit in KS tissue (69). Furthermore, a small molecule inhibitor of tyrosine kinase activity, STI 571 (Gleevec) that inhibits c-Kit activity (50) was available to examine a role for c-Kit in our in vitro system. c-Kit induction in KSHV-infected DMVEC was confirmed at the mRNA level by quantitative real-time PCR (Table 2) and at the protein level by immunofluorescence analysis (IFA) (Fig. 2A). To verify that c-Kit induction was independent of endothelial cell immortalization, IFA was also performed on primary DMVEC infected with a recombinant KSHV strain expressing GFP (110). In agreement with our previous observations, enhanced expression of c-Kit was observed on GFP-positive, KSHV-infected cells in the virus-exposed culture, but not on adjacent GFP-negative uninfected cells (Fig. 2B).

Other studies have shown that endothelial cells from umbilical vein and aorta coexpress c-Kit and the SCF ligand (8, 16, 19, 113). To determine whether DMVEC expressed SCF in addition to c-Kit, we performed real-time RT-PCR analysis for SCF mRNA. The ratios for SCF-RNA levels in the four infected samples used in our real-time PCR analysis compared to the corresponding mock-infected cells are shown in Table 2. In contrast to c-Kit, there was no general tendency of SCF upregulation in KSHV-infected DMVEC. Due to alternative RNA splicing, the SCF protein exists in both membrane-bound and soluble forms (41). We thus performed RT-PCR using isoform-specific primers to directly distinguish between membrane-bound and soluble SCF transcripts (49). Analysis of the RT-PCR products by agarose gel electrophoresis indicated that the ratio of membrane-bound to soluble SCF in DMVEC is also unaffected by KSHV infection (data not shown). Moreover, analysis of DMVEC culture supernatants using a SCF-specific ELISA to measure secretion of SCF showed no significant changes in protein levels associated with KSHV infection (data not shown). Thus, if KSHV infection alters c-Kit/SCF-regulated signaling pathways, the contribution of virus infection is presumably at the level of c-Kit expression.

c-Kit expression in KSHV-infected DMVEC promotes proliferation in response to exogenous SCF. To examine whether KSHV-induced upregulation of c-Kit had functional consequences, we tested whether the mitogenic response of DMVEC to exogenous SCF was enhanced following KSHV infection. Mock- and KSHV-infected DMVEC were cultured in growth factor depleted medium in the absence and presence of recombinant SCF and proliferation was measured using an XTT-based dye reduction assay (88). Both mock- and KSHV-infected DMVEC exhibited a dose-dependent proliferation in response to exogenous SCF that was maximal at 50 to 100 ng/ml. However, infected DMVEC were significantly more responsive to exogenous ligand than mock-infected DMVEC (Fig. 3A). In mock-infected cultures, the increase over basal proliferation in the absence of recombinant SCF was never more than 40%, while proliferation of KSHV-infected DMVEC was increased by as much as 85%. During KS disease, an enhanced capacity of KSHV-infected endothelial cells to respond to SCF produced by adjacent endothelial cells, or by macrophages and mast cells infiltrating the KS lesion, would promote more rapid growth of virus-infected cells.

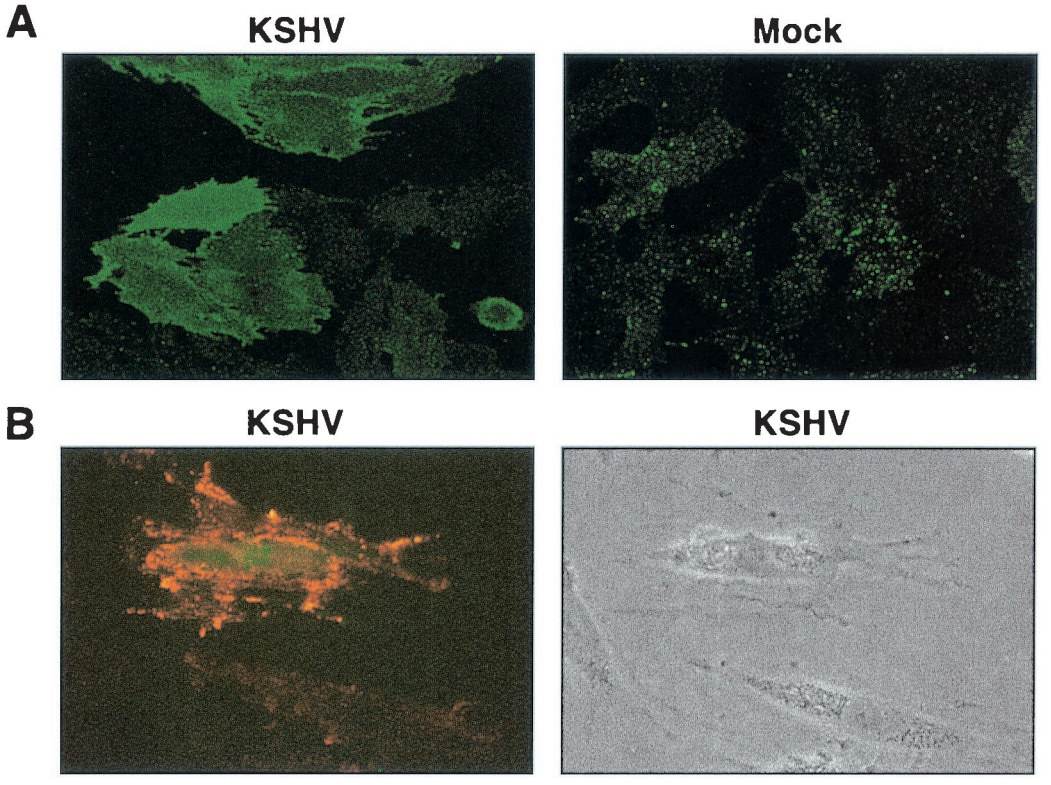

FIG. 2. Induction of c-Kit protein on immortalized and primary DMVEC following KSHV infection. (A) Immunofluorescence microscopy illustrating upregulation of c-Kit protein on the surface of E6/E7-immortalized KSHV-infected DMVEC monolayers (KSHV). In contrast, low levels of constitutive c-Kit expression were detected on mock-infected monolayers (Mock). Cells were stained for c-Kit at 3 weeks p.i., when ±60% of the culture was KSHV-infected. (B) Immunofluorescence microscopy illustrating induction of c-Kit (red) on the surface of pDMVEC infected with GFP-KSHV (green) relative to constitutive levels of c-Kit expressed on adjacent uninfected cells in the same monolayer. The corresponding phase image is also shown. Cells were stained for c-Kit at 1 week p.i., when <50% of the cells were KSHV-infected. GFP expression indicates the KSHV-infected cell in the dark-field image.

The c-Kit tyrosine kinase inhibitor STI 571 inhibits the proliferation of KSHV-infected DMVEC. To further substantiate a role for c-Kit/SCF in the enhanced growth response of KSHV-infected DMVEC, proliferation of infected DMVEC in response to exogenous SCF was measured in the presence of increasing concentrations of an inhibitor of c-Kit tyrosine kinase activity, STI 571. STI 571 (Gleevec) was designed as an ATP-competitive inhibitor of the Abl tyrosine kinase (17, 18, 35) and was later shown to be active against c-Kit (50). As illustrated in Fig. 3B, the proliferative response of KSHV-infected DMVEC to exogenous SCF was completely inhibited by a 1 μM dose of STI 571. Testing of DMVEC viability by trypan blue exclusion showed that growth inhibition was not due to nonspecific cytotoxicity of STI 571 (data not shown). In addition, STI 571 had no effect on the capacity of the human Jurkat T-cell line to proliferate in response to exogenous IL-2 (data not shown). The capacity of STI 571 to inhibit KSHV-infected DMVEC proliferation confirms a role for c-Kit signaling in the growth response of KSHV-infected cells and further suggests a novel strategy for KS therapy.

Inhibition of c-Kit activity reverses KSHV-induced transformation. Induction of growth signaling loops is a frequently described consequence of abnormal c-Kit/SCF activity in tumor cell lines. In addition, enhanced c-Kit expression has been associated with changes in cell morphology and acquisition of a transformed phenotype (1, 21, 61). We previously demonstrated that KSHV-infected DMVEC develop a spindle phenotype and exhibit transformed characteristics including disorganized growth, focus formation and anchorage-independent growth in semisolid agar (71). To examine whether KSHV-induction of c-Kit also plays a role in virus-induced cell spindling and transformation, the consequence of inhibiting c-Kit signaling in KSHV-transformed DMVEC was evaluated. As illustrated in Fig. 4A, KSHV-transformed DMVEC exhibit disorganized growth, loss of contact inhibition and focus formation in monolayer culture. However, following treatment of DMVEC with STI 571 to inhibit endogenous c-Kit tyrosine kinase activity, focus formation was inhibited and an organized monolayer with distinct cell margins was reestablished. The effect of STI 571 was dose dependent and complete at a drug concentration of 1 μM. The loss of transformed growth characteristics was not due to drug-induced cytotoxicity since removal of STI 571 led to regeneration of the transformed phenotype, even after exposure of cells to a 10 μM dose (data not shown). Uninfected DMVEC exhibited normal growth with an organized cobblestone phenotype when maintained at confluency, and exposure to STI 571 had no effect on cell morphology or viability (data not shown).

Because STI 571 is also active against the Abl and platelet-derived growth factor (PDGF) β receptor tyrosine kinases (18,

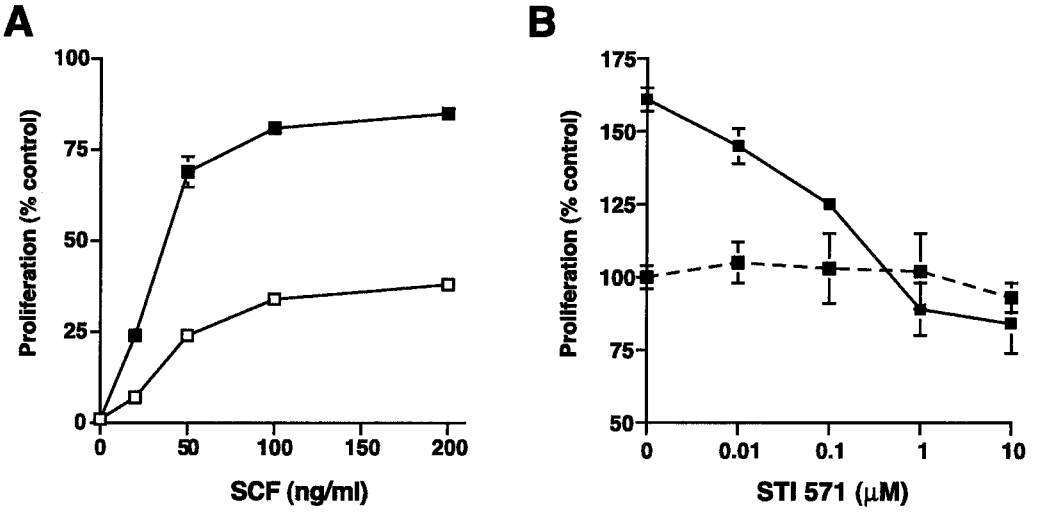

FIG. 3. SCF-dependent proliferation of DMVEC is enhanced by KSHV infection. (A) Proliferative response of mock (open squares)- and KSHV (filled squares)-infected DMVEC to exogenous SCF. Proliferation was measured using an XTT-based assay. Results from triplicate wells (± standard deviations [error bars]) are expressed as the percentage increase over basal proliferation measured in the absence of exogenous SCF. Representative results from one of three independent experiments are shown. (B) An inhibitor of c-Kit tyrosine kinase activity (STI 571) eliminates SCF-dependent DMVEC proliferation. KSHV-infected DMVEC were cultured in the presence of increasing doses of STI 571 and in the presence (solid line) or absence (dashed line) of exogenous SCF (50 ng/ml). Proliferation of KSHV-infected DMVEC was measured with an XTT-based assay as described above, but STI 571 was added at the same time as SCF (50 ng/ml). Results for triplicate wells (± standard deviations [error bars]) are expressed as a percentage of basal proliferation measured in the absence of SCF and STI 571 (expressed as 100%). Representative results from one of three independent experiments are shown.

35), the inhibitory activity in DMVEC could imply a role for one or other of these receptors in KSHV-induced transformation. DNA microarray analysis of DMVEC did not reveal any KSHV-induced upregulation of Abl, PDGF or PDGF-receptor genes, suggesting that c-Kit was the primary drug target. However, to confirm a central role for c-Kit in KSHV-induced DMVEC transformation, we designed a complementary approach to specifically inhibit c-Kit signaling in KSHV-transformed DMVEC. In this approach, a dominant negative c-Kit protein (c-Kit DN) lacking the cytoplasmic ATP-binding and phosphotransferase domains necessary for c-Kit signaling was expressed in DMVEC using a previously described adenovirus delivery system (101). KSHV-infected DMVEC that exhibited pronounced focus formation were infected with an adenovirus vector expressing c-Kit DN (Ad/c-KitDN) along with an adenovirus expressing a transactivator (Ad/trans) necessary for induction of c-Kit gene expression. To control for infection efficiency and nonspecific effects of adenovirus infection, parallel DMVEC cultures were infected with an adenovirus expressing green fluorescent protein (Ad/GFP) and Ad/trans. In control cultures, these GFP were expressed at high levels in the majority of DMVEC but no change in the transformed phenotype was observed (data not shown). In contrast, expression of the dominant negative c-Kit protein in KSHV-transformed DMVEC resulted in a dramatic loss of transformed foci with cells flattening out and becoming organized in a manner identical to that observed following STI 571 treatment (Fig. 4B). The ability to reverse KSHV-induced morphological transformation through specific inhibition of c-Kit activity demonstrates a critical role for c-Kit signaling in KSHV-induced transformation of endothelial cells and supports a role for upregulation of c-Kit as a factor in KS tumorigenesis.

Expression of c-Kit in DMVEC is sufficient for induction of morphological transformation. Ectopic expression of c-Kit in murine fibroblasts induces morphological alteration, growth in soft agar and tumorigenicity in nude mice (1, 21, 61). To determine whether c-Kit upregulation was sufficient to induce the morphological changes caused by KSHV infection, c-Kit was overexpressed in normal DMVEC in the absence of KSHV infection. The c-Kit overexpression was achieved by infecting DMVEC with an adenovirus vector expressing wild type c-Kit protein (Ad/c-KitWT) along with the adenovirus transactivator (Ad/trans) as described above. As illustrated in Fig. 5, c-Kit overexpression had a dose-dependent effect on DMVEC morphology that was highly reminiscent of that observed following KSHV infection. Ad/c-KitWT-infected cells became spindle-shaped and disorganized, with overgrowth of the monolayer and a loss of discrete cell borders. Morphological changes were first noted at day 5 postinfection (p.i.) and were prominent by day 10 p.i.. The changes were specific to adenovirus-infected cultures overexpressing c-Kit, since DMVEC infected with Ad/GFP were maintained for up to three weeks without phenotypic alteration. Immunofluorescent staining was performed on DMVEC infected with Ad/c-KitWT at a low MOI (MOI of 10) by use of an anti-c-Kit MAB followed by a FITC-conjugate to confirm that spindle formation was restricted to those cells that expressed high levels of c-Kit protein on the cell surface. Addition of exogenous SCF to Ad/GFP- or Ad/c-KitWT-infected DMVEC did not induce or accentuate morphological change, and adenovirus infection did not alter SCF production by DMVEC (data not shown). These results suggest that the endogenous SCF produced by DMVEC is sufficient to activate the pathways leading to morphological transformation. Importantly, these studies demon-

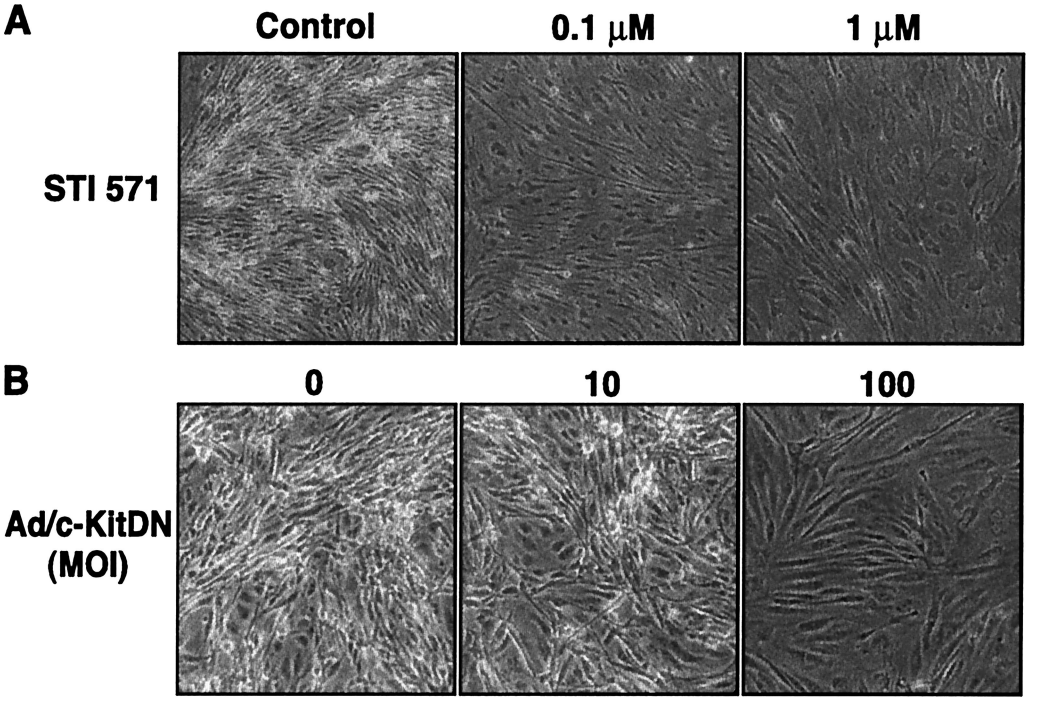

FIG. 4. Inhibition of c-Kit tyrosine kinase activity reverses the transformed phenotype of KSHV-infected DMVEC. (A) KSHV-infected DMVEC exhibiting disorganized growth and focus formation were left untreated (Control) or treated with STI 571 (0.1 and 1 μM) for 5 days. The STI 571-induced focus loss and monolayer reorganization were observed and recorded with a Nikon light microscope. (B) KSHV-infected DMVEC exhibiting disorganized growth and focus formation were left untreated (0) or infected with an adenovirus vector expressing a dominant negative c-Kit protein (Ad/c-KitDN) at an MOI of 10 or 100 for 5 days, and the elimination of focus formation was recorded as for panel A. For both the pharmacological and dominant negative protein inhibition protocols, results from one of three independent experiments are shown. Fields photographed were representative of the entire monolayer of treated cells.

strate that increased expression of c-Kit in DMVEC is sufficient to induce morphological changes comparable to those observed following KSHV infection of DMVEC.

DISCUSSION

DNA microarrays permit a global look at the transcriptional changes occurring during biological process such as carcinogenesis. One of the most promising applications for this technology is the classification of cancer and the dissection of molecular mechanisms of tumor progression (25, 32, 48, 52, 83). However, the identification of transcriptional changes also suggests novel possibilities for intervention. Since there is currently no known treatment for KS, our finding that upregulation of c-*kit* expression by KSHV is not only necessary but also sufficient for endothelial cell transformation suggests that the pharmacological inhibitor STI 571 (Gleevec) can be used to treat KS. STI 571 was recently approved by the U.S. Food and Drug Administration for the treatment of gastrointestinal stromal tumor (GIST), where c-Kit is the effective target, and is in clinical trials for the treatment of small cell lung cancer (SCLC) where inhibition of c-Kit signaling successfully arrests the growth of SCLC cells in vitro (59, 111). Our study demonstrates the successful convergence of different technologies to enable transition from a complex in vitro model of viral pathogenesis to identification of relevant cellular genes that may constitute valid therapeutic targets.

The experimental system used here relied largely on KSHV-infected DMVEC cells that were immortalized with the E6 and E7 genes of HPV type 16 prior to KSHV infection. As we demonstrated earlier, the immortalized DMVEC retain expression of endothelial cell markers, grow as a cobblestone monolayer, and do not exhibit abnormal growth factor requirements (71). Moreover, this approach allowed us to compare infected and noninfected cell lines grown in parallel for the same time period, thus allowing for time-matched controls. However, since any E6/E7-induced changes in cellular gene profiles are controlled for by the relative comparison with mock-infected control cells, our analysis will not reveal genes regulated commonly by KSHV and E6/E7. Recently, Poole et al. compared the transcriptional profile of DMVEC transformed with KSHV to nontransformed primary DMVEC using Atlas DNA filter arrays and Incyte cDNA spotted arrays (80). Of the 124 genes that were upregulated in our study, Poole and colleagues confirmed RDC-1 and LMO2 by RT-PCR and 5 additional genes by array analysis (MEF2C, LGALS9, GJA1, IL-1R1, and SCYA14). Of the 60 downregulated genes in our study, Poole and colleagues confirmed 3 genes by array analysis (SDF1, PLAU, and TXNRD1). MCP-1 was found to be repressed in the study by Poole et al. However, our real-time PCR analysis confirmed MCP-1 upregulation in our experimental system. Similarly, UBE2C was upregulated in our study but downregulated in the Poole et al. study. With these two exceptions, genes that changed significantly in both studies

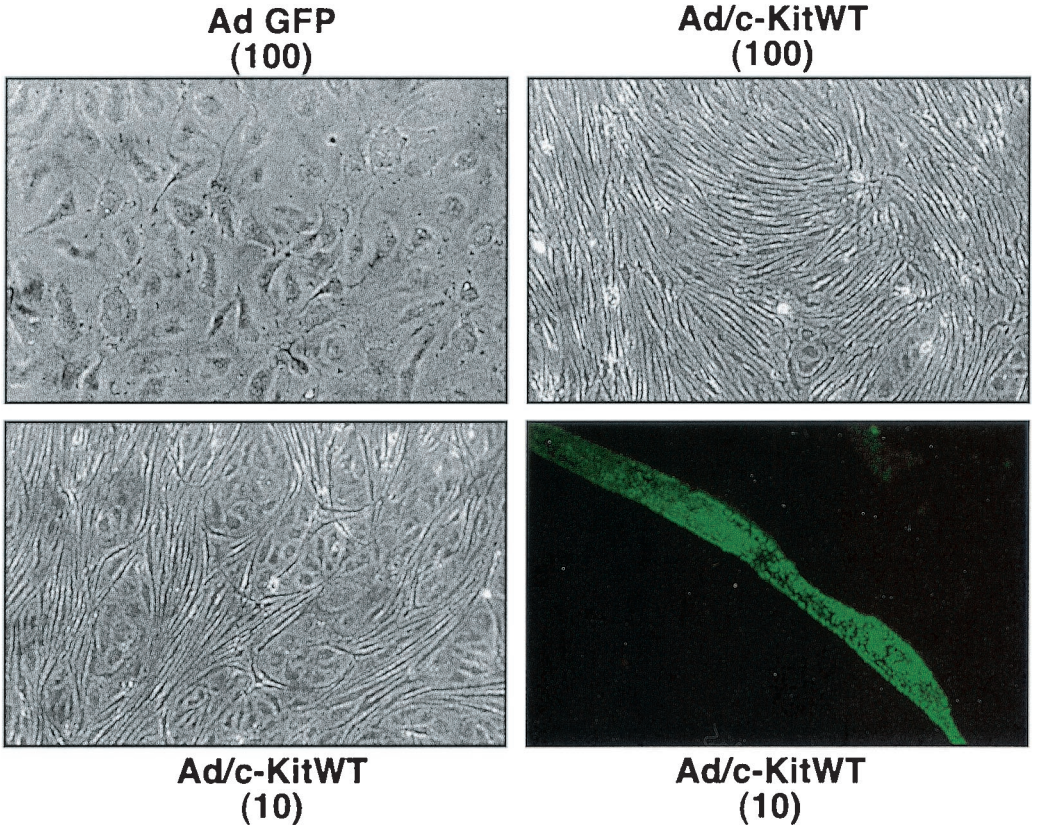

FIG. 5. Ectopic expression of c-Kit in normal DMVEC induces morphological changes. DMVEC monolayers infected with a control adenovirus vector expressing GFP (Ad/GFP) at an MOI of 100 maintain a normal cobblestone morphology. In contrast, DMVEC infected with a recombinant adenovirus expressing c-Kit (Ad/c-KitWT) exhibit spindle morphology and disorganized growth. A dose-dependent effect was observed in DMVEC monolayers infected with Ad/c-KitWT at an MOI of 10, supporting the argument for a direct effect of c-Kit on spindle formation. This was confirmed by immunofluorescence microscopy on monolayers infected with Ad/c-KitWT at an MOI of 10. The dark-field enlargement illustrates strong expression of c-Kit protein specifically on a cell exhibiting spindle morphology.

showed the same tendency of up- or downregulation suggesting that each system identifies KSHV-regulated genes reliably.

In addition to genes that were changed in both experiments, each analysis identified genes that did not change or were not examined in the other assay. Of the remaining genes changing significantly in our analysis, 117 were not present on the cDNA arrays used by Poole et al. (http://pc190-10.kennedykrieger.org/microarraydata/). All other genes (57) were not observed to change in their study. Of the 313 genes that changed in the Poole et al. study, 96 were also tested in our system. Of these genes, 19 changed significantly in at least one of the infected cell lines. A possible reason for these discrepancies is that many more factors contribute to the exclusion of genes from this type of analysis than to their inclusion. For instance, although repeat experiments will dramatically lower the rate of false positives, they will not decrease the number of false negatives at the same rate, since signals that are not detected because of poor probe design will not become apparent simply by repeating the experiment. However, it is also possible that genes were excluded from our study because they were also altered due to E6/E7 expression. For example, transcriptional profiling of HPV-transformed keratinocytes has identified STAT-1 as one of the major downregulated genes with the consequence of a strong repression of the interferon-response genes (29). In contrast to Poole et al., we did not observe a strong induction of interferon-regulated genes upon KSHV infection. Since the same DNA array was able to detect ISG-induction by HCMV (97), we should have detected changes in ISG messages. A possible explanation could thus be that E6 and E7 counteract the interferon-inducing activity of KSHV.

Importantly, the dramatic transformation of endothelial cells, as evidenced by the change from a monolayer cobblestone phenotype to focus-forming spindle cell phenotype, was reflected in the large number of transcriptional changes over and above any changes due to E6/E7-immortalization. Particularly relevant to this process seems to be the large number of genes with known functions in cell proliferation and differentiation. One of the genes that was consistently upregulated and appeared to be a good candidate to test this assumption was c-*kit*. The upregulation of c-*kit* by KSHV was observed both in immortalized as well as primary DMVEC (Fig. 2). This further supports the use of the immortalized DMVEC to identify KSHV-induced cellular genes.

While c-Kit expression and c-Kit–SCF interactions are crucial for the normal development of hematopoietic cells and a restricted number of nonhematopoietic cells, expression of c-Kit has also been associated with a number of malignancies.

In these c-Kit-associated malignancies, although distinct mutations of the c-Kit molecule are involved, all appear to be associated with an increased activity of the c-Kit/SCF signaling pathway. For example, in GISTs and germ cell neoplasms, gain-of-function mutations in juxtamembrane and tyrosine kinase domains have been described which permit, respectively, ligand-independent dimerization or constitutive activation without dimerization (53, 66, 76, 107). In SCLC and breast cancer, the observed coexpression of c-Kit and SCF is thought to generate an autocrine growth loop (51, 56, 58, 68, 109). As endothelial cells are the precursors of KS spindle cells, our finding that KSHV infection of dermal endothelial cells enhances c-Kit expression with a concomitant increase in c-Kit signaling activity indicates that c-Kit expression may also play an important role in the development and progression of KS. A recent study evaluating c-Kit expression in frozen samples of KS tissue by immunohistochemistry identified c-Kit expression in 2 of 13 samples examined (69). However, since fresh tissue was not available for examination by complementary methods or optimized histochemical procedures, c-Kit expression in additional samples may have been beyond the limits of detection. In addition, no information was presented regarding the clinical staging of the tumor tissue or the presence or activation state of the KSHV genome. Consequently, detection of c-Kit expression in at least some of the archival tissue studied supports an involvement for c-Kit expression in KS pathogenesis.

Our data demonstrate that both mock- and KSHV-infected DMVEC proliferate in response to exogenous SCF. However, the proliferative response to SCF was significantly greater in the KHSV-infected DMVEC than in uninfected cells. The more moderate response of uninfected DMVEC to exogenous SCF suggests that the level of c-Kit expression may be rate limiting for growth. In addition, stimulation of c-Kit by endogenous SCF and auxiliary regulation of receptor activity may also modulate proliferation. Similar observations on the proliferative response to exogenous SCF have been made for other cell types that coexpress c-Kit and SCF (51, 58, 109). For example, in a study of SCF-positive breast tumor subclones engineered to express different levels of c-Kit, only the cells expressing the highest levels of c-Kit responded to exogenous SCF (51). In our studies, the enhanced proliferative response of KHSV-infected DMVEC to SCF suggests that KSHV infection induces c-Kit expression to a level that enables an increased responsiveness to exogenous SCF.

In other cell systems, the c-Kit/SCF signaling pathway has been shown to play a role in cellular transformation as well as growth dysregulation. GISTs, which are though to originate from the interstitial cells of Cajal and are characterized by expression of c-Kit, commonly have a spindle cell or mixed epitheloid-spindle cell morphology (2). Also, ectopic expression of c-Kit in murine fibroblasts allows disorganized cell growth, loss of contact inhibition, and focus formation (1, 21, 61). Notably, such changes are reminiscent of those we have observed in KSHV-infected DMVEC (71). In GISTs, c-Kit mutations allow ligand-independent activation, while in the murine fibroblast system, exogenous ligand is required to induce transformation. In our DMVEC studies, the coexpression of SCF appears to facilitate an autocrine effect. The ability to reverse KSHV-induced phenotypic changes in DMVEC by inhibition of c-Kit tyrosine kinase activity strongly suggests that autocrine c-Kit/SCF interactions, in the context of increased c-Kit expression, play a role in cellular transformation. Furthermore, the phenotypic changes observed in DMVEC following c-Kit overexpression in the absence of KSHV infection further implicate KSHV-induced enhancement of c-Kit expression as a crucial event in DMVEC transformation.

Identification of a causative role for c-Kit in KSHV-associated cellular transformation suggests a novel therapeutic target for KS. The STI 571, the c-Kit tyrosine kinase inhibitor described in this report, is approved for the treatment of chronic myelogenous leukemia, a disease associated with BCR-ABL kinase activity, and GIST, a disease associated with constitutive c-Kit activation. In conclusion, c-Kit should be considered a primary target in KS tumorigenesis. Consequently, STI 571, or other pharmacological inhibitors of c-Kit signaling, should be evaluated as potential therapeutic agents for the treatment of KS.

ACKNOWLEDGMENTS

We thank the R. W. Johnson PRI Microarray Core and Bioinformatics Facility for performing the array analysis. We also thank Veena Rajaraman and Jeff King for help with the data analysis. We thank Jeffrey Vieira (Fred Hutchinson Cancer Research Center) for providing the recombinant GFP-KSHV and Bala Chandran (University of Kansas Medical Center, Kansas City) for providing anti-KSHV antibodies. We thank Franziska Ruchti for assistance in preparing samples for array analysis and Andrew Townsend for assistance with manuscript preparation.

This work was supported in part by a core grant from the Oregon National Primate Research Center (RR00163) (A.V.M. and K.F.).

REFERENCES

1. **Alexander, W. S., S. D. Lyman, and E. F. Wagner.** 1991. Expression of functional c-kit receptors rescues the genetic defect of W mutant mast cells. EMBO J. **10:**3683–3691.
2. **Allander, S. V., N. N. Nupponen, M. Ringner, G. Hostetter, G. W. Maher, N. Goldberger, Y. Chen, J. Carpten, A. G. Elkahloun, and P. S. Meltzer.** 2001. Gastrointestinal stromal tumors with KIT mutations exhibit a remarkably homogeneous gene expression profile. Cancer Res. **61:**8624–8628.
3. **Aluigi, M. G., A. Albini, S. Carlone, L. Repetto, R. De Marchi, A. Icardi, M. Moro, D. Noonan, and R. Benelli.** 1996. KSHV sequences in biopsies and cultured spindle cells of epidemic, iatrogenic and Mediterranean forms of Kaposi's sarcoma. Res. Virol. **147:**267–275.
4. **Ambroziak, J. A., D. J. Blackbourn, B. G. Herndier, R. G. Glogau, J. H. Gullett, A. R. McDonald, E. T. Lennette, and J. A. Levy.** 1995. Herpes-like sequences in HIV-infected and uninfected Kaposi's sarcoma patients. Science **268:**582–583.
5. **Aoki, Y., E. S. Jaffe, Y. Chang, K. Jones, J. Teruya-Feldstein, P. S. Moore, and G. Tosato.** 1999. Angiogenesis and hematopoiesis induced by Kaposi's sarcoma-associated herpesvirus-encoded interleukin-6. Blood **93:**4034–4043.
6. **Argiles, J. M., and F. J. Lopez-Soriano.** 2001. Insulin and cancer. Int. J. Oncol. **18:**683–687.
7. **Arvanitakis, L., E. A. Mesri, R. G. Nador, J. W. Said, A. S. Asch, D. M. Knowles, and E. Cesarman.** 1996. Establishment and characterization of a primary effusion (body cavity-based) lymphoma cell line (BC-3) harboring Kaposi's sarcoma-associated herpesvirus (KSHV/HHV-8) in the absence of Epstein-Barr virus. Blood **88:**2648–2654.
8. **Aye, M. T., S. Hashemi, B. Leclair, A. Zeibdawi, E. Trudel, M. Halpenny, V. Fuller, and G. Cheng.** 1992. Expression of stem cell factor and c-kit mRNA in cultured endothelial cells, monocytes and cloned human bone marrow stromal cells (CFU-RF). Exp. Hematol. **20:**523–527.
9. **Bais, C., B. Santomasso, O. Coso, L. Arvanitakis, E. G. Raaka, J. S. Gutkind, A. S. Asch, E. Cesarman, M. C. Gershengorn, E. A. Mesri, and M. C. Gerhengorn.** 1998. G-protein-coupled receptor of Kaposi's sarcoma-associated herpesvirus is a viral oncogene and angiogenesis activator. Nature **391:**86–89.
10. **Bayes-Genis, A., C. A. Conover, and R. S. Schwartz.** 2000. The insulin-like growth factor axis: a review of atherosclerosis and restenosis. Circ. Res. **86:**125–130.
11. **Beckstead, J. H., G. S. Wood, and V. Fletcher.** 1985. Evidence for the origin

of Kaposi's sarcoma from lymphatic endothelium. Am. J. Pathol. **119:**294–300.
12. **Boissan, M., F. Feger, J. J. Guillosson, and M. Arock.** 2000. c-Kit and c-kit mutations in mastocytosis and other hematological diseases. J. Leukoc. Biol. **67:**135–148.
13. **Boshoff, C., Y. Endo, P. D. Collins, Y. Takeuchi, J. D. Reeves, V. L. Schweickart, M. A. Siani, T. Sasaki, T. J. Williams, P. W. Gray, P. S. Moore, Y. Chang, and R. A. Weiss.** 1997. Angiogenic and HIV-inhibitory functions of KSHV-encoded chemokines. Science (Washington, D.C.) **278:**290–294.
14. **Boshoff, C., S.-J. Gao, L. E. Healy, S. Matthews, A. J. Thomas, L. Coignet, R. A. Warnke, J. A. Strauchen, E. Matutes, O. W. Karnel, P. S. Moore, R. A. Weiss, and Y. Chang.** 1998. Establishing a KSHV+ cell line (BCP-1) from peripheral blood and characterizing its growth in nod/SCID mice. Blood **91:**1671–1679.
15. **Boshoff, C., T. F. Schulz, M. M. Kennedy, A. K. Graham, C. Fisher, A. Thomas, J. O. McGee, R. A. Weiss, and J. J. O'Leary.** 1995. Kaposi's sarcoma-associated herpesvirus infects endothelial and spindle cells. Nat. Med. **1:**1274–1278.
16. **Broudy, V. C., N. L. Kovach, L. G. Bennett, N. Lin, F. W. Jacobsen, and P. G. Kidd.** 1994. Human umbilical vein endothelial cells display high-affinity c-kit receptors and produce a soluble form of the c-kit receptor. Blood **83:**2145–2152.
17. **Buchdunger, E., J. Zimmermann, H. Mett, T. Meyer, M. Muller, B. J. Druker, and N. B. Lydon.** 1996. Inhibition of the Abl protein-tyrosine kinase in vitro and in vivo by a 2-phenylaminopyrimidine derivative. Cancer Res. **56:**100–104.
18. **Buchdunger, E., J. Zimmermann, H. Mett, T. Meyer, M. Muller, U. Regenass, and N. B. Lydon.** 1995. Selective inhibition of the platelet-derived growth factor signal transduction pathway by a protein-tyrosine kinase inhibitor of the 2-phenylaminopyrimidine class. Proc. Natl. Acad. Sci. USA **92:**2558–2562.
19. **Buzby, J. S., E. M. Knoppel, and M. S. Cairo.** 1994. Coordinate regulation of Steel factor, its receptor (Kit), and cytoadhesion molecule (ICAM-1 and ELAM-1) mRNA expression in human vascular endothelial cells of differing origins. Exp. Hematol. **22:**122–129.
20. **Cannon, J., F. Hamzeh, S. Moore, J. Nicholas, and R. Ambinder.** 1999. Human herpesvirus 8-encoded thymidine kinase and phosphotransferase homologues confer sensitivity to ganciclovir. J. Virol. **73:**4786–4793.
21. **Caruana, G., A. C. Cambareri, T. J. Gonda, and L. K. Ashman.** 1998. Transformation of NIH3T3 fibroblasts by the c-Kit receptor tyrosine kinase: effect of receptor density and ligand-requirement. Oncogene **16:**179–190.
22. **Cesarman, E., Y. Chang, P. S. Moore, J. W. Said, and D. M. Knowles.** 1995. Kaposi's sarcoma-associated herpesvirus-like DNA sequences in AIDS-related body-cavity-based lymphomas. N. Engl. J. Med. **332:**1186–1191.
23. **Cesarman, E., R. G. Nador, F. Bai, R. A. Bohenzky, J. J. Russo, P. S. Moore, Y. Chang, and D. M. Knowles.** 1996. Kaposi's sarcoma-associated herpesvirus contains G protein-coupled receptor and cyclin D homologs which are expressed in Kaposi's sarcoma and malignant lymphoma. J. Virol. **70:**8218–8223.
24. **Chan, S. R., C. Bloomer, and B. Chandran.** 1998. Identification and characterization of human herpesvirus-8 lytic cycle-associated ORF 59 protein and the encoding cDNA by monoclonal antibody. Virology **240:**118–126.
25. **Chan, W. C., and J. Z. Huang.** 2001. Gene expression analysis in aggressive NHL. Ann. Hematol. **80:**B38–41.
26. **Chandran, B., C. Bloomer, S. R. Chan, L. Zhu, E. Goldstein, and R. Horvat.** 1998. Human herpesvirus-8 ORF K8.1 gene encodes immunogenic glycoproteins generated by spliced transcripts. Virology **249:**140–149.
27. **Chang, Y., E. Cesarman, M. S. Pessin, F. Lee, J. Culpepper, D. M. Knowles, and P. S. Moore.** 1994. Identification of herpesvirus-like DNA sequences in AIDS-associated Kaposi's sarcoma. Science **266:**1865–1869.
28. **Chang, Y., P. S. Moore, S. J. Talbot, C. H. Boshoff, T. Zarkowska, K. Godden, H. Paterson, R. A. Weiss, and S. Mittnacht.** 1996. Cyclin encoded by KS herpesvirus. Nature **382:**410.
29. **Chang, Y. E., and L. A. Laimins.** 2000. Microarray analysis identifies interferon-inducible genes and Stat-1 as major transcriptional targets of human papillomavirus type 31. J. Virol. **74:**4174–4182.
30. **Cheng, E. H., J. Nicholas, D. S. Bellows, G. S. Hayward, H. G. Guo, M. S. Reitz, and J. M. Hardwick.** 1997. A Bcl-2 homolog encoded by Kaposi sarcoma-associated virus, human herpesvirus 8, inhibits apoptosis but does not heterodimerize with Bax or Bak. Proc. Natl. Acad. Sci. USA **94:**690–694.
31. **Ciufo, D. M., J. S. Cannon, L. J. Poole, F. Y. Wu, P. Murray, R. F. Ambinder, and G. S. Hayward.** 2001. Spindle cell conversion by Kaposi's sarcoma-associated herpesvirus: formation of colonies and plaques with mixed lytic and latent gene expression in infected primary dermal microvascular endothelial cell cultures. J. Virol. **75:**5614–5626.
32. **Clarke, P. A., R. te Poele, R. Wooster, and P. Workman.** 2001. Gene expression microarray analysis in cancer biology, pharmacology, and drug development: progress and potential. Biochem. Pharmacol. **62:**1311–1336.
33. **Damania, B., and J. U. Jung.** 2001. Comparative analysis of the transforming mechanisms of Epstein-Barr virus, Kaposi's sarcoma-associated herpesvirus, and Herpesvirus saimiri. Adv. Cancer Res. **80:**51–82.
34. **Davis, M. A., M. A. Sturzl, C. Blasig, A. Schreier, H. G. Guo, M. Reitz, S. R. Opalenik, and P. J. Browning.** 1997. Expression of human herpesvirus 8-encoded cyclin D in Kaposi's sarcoma spindle cells. J. Natl. Cancer Inst. **89:**1868–1874.
35. **Druker, B. J., S. Tamura, E. Buchdunger, S. Ohno, G. M. Segal, S. Fanning, J. Zimmermann, and N. B. Lydon.** 1996. Effects of a selective inhibitor of the Abl tyrosine kinase on the growth of Bcr-Abl positive cells. Nat. Med. **2:**561–566.
36. **Dupin, N., C. Fisher, P. Kellam, S. Ariad, M. Tulliez, N. Franck, E. Van Marck, D. Salmon, I. Gorin, J.-P. Escande, R. A. Weiss, K. Alitalo, and C. Boshoff.** 1999. Distribution of human herpesvirus-8 latently infected cells in Kaposi's sarcoma, multicentric Castleman's disease, and primary effusion lymphoma. Proc. Natl. Acad. Sci. USA **96:**4546–4551.
37. **Ensoli, B., and M. C. Sirianni.** 1998. Kaposi's sarcoma pathogenesis: a link between immunology and tumor biology. Crit. Rev. Oncog. **9:**107–124.
38. **Erickson, J. W., and R. A. Cerione.** 2001. Multiple roles for Cdc42 in cell regulation. Curr. Opin. Cell Biol. **13:**153–157.
39. **Fajas, L., M. B. Debril, and J. Auwerx.** 2001. Peroxisome proliferator-activated receptor-gamma: from adipogenesis to carcinogenesis. J. Mol. Endocrinol. **27:**1–9.
40. **Febbraio, M., D. P. Hajjar, and R. L. Silverstein.** 2001. CD36: a class B scavenger receptor involved in angiogenesis, atherosclerosis, inflammation, and lipid metabolism J. Clin. Invest. **108:**785–791.
41. **Flanagan, J. G., D. C. Chan, and P. Leder.** 1991. Transmembrane form of the kit ligand growth factor is determined by alternative splicing and is missing in the Sld mutant. Cell **64:**1025–1035.
42. **Flore, O., S. Rafii, S. Ely, J. J. O'Leary, E. M. Hyjek, and E. Cesarman.** 1998. Transformation of primary human endothelial cells by Kaposi's sarcoma-associated herpesvirus. Nature **394:**588–592.
43. **Früh, K., K. Simmen, B. G. M. Luukkonen, Y. C. Bell, and P. Ghazal.** 2001. Virogenomics: a novel approach to antiviral drug discovery. Drug Disc. Today **6:**601–608.
44. **Gao, S. J., C. Boshoff, S. Jayachandra, R. A. Weiss, Y. Chang, and P. S. Moore.** 1997. KSHV ORF K9 (vIRF) is an oncogene which inhibits the interferon signaling pathway. Oncogene **15:**1979–1985.
45. **Graham, D. K., G. W. Bowman, T. L. Dawson, W. L. Stanford, H. S. Earp, and H. R. Snodgrass.** 1995. Cloning and developmental expression analysis of the murine c-mer tyrosine kinase. Oncogene **10:**2349–2359.
46. **Grimberg, A., and P. Cohen.** 2000. Role of insulin-like growth factors and their binding proteins in growth control and carcinogenesis. J. Cell. Physiol. **183:**1–9.
47. **Guo, H. G., P. Browning, J. Nicholas, G. S. Hayward, E. Tschachler, Y. W. Jiang, M. Sadowska, M. Raffeld, S. Colombini, R. C. Gallo, and M. S. Reitz, Jr.** 1997. Characterization of a chemokine receptor-related gene in human herpesvirus 8 and its expression in Kaposi's sarcoma. Virology **228:**371–378.
48. **Hegde, P., R. Qi, R. Gaspard, K. Abernathy, S. Dharap, J. Earle-Hughes, C. Gay, N. U. Nwokekeh, T. Chen, A. I. Saeed, V. Sharov, N. H. Lee, T. J. Yeatman, and J. Quackenbush.** 2001. Identification of tumor markers in models of human colorectal cancer using a 19,200-element complementary DNA microarray. Cancer Res. **61:**7792–7797.
49. **Heinrich, M. C., D. C. Dooley, A. C. Freed, L. Band, M. E. Hoatlin, W. W. Keeble, S. T. Peters, K. V. Silvey, F. S. Ey, D. Kabat, et al.** 1993. Constitutive expression of steel factor gene by human stromal cells. Blood **82:**771–783.
50. **Heinrich, M. C., D. J. Griffith, B. J. Druker, C. L. Wait, K. A. Ott, and A. J. Zigler.** 2000. Inhibition of c-kit receptor tyrosine kinase activity by STI 571, a selective tyrosine kinase inhibitor. Blood **96:**925–932.
51. **Hines, S. J., C. Organ, M. J. Kornstein, and G. W. Krystal.** 1995. Coexpression of the c-kit and stem cell factor genes in breast carcinomas. Cell Growth Differ. **6:**769–779.
52. **Hippo, Y., H. Taniguchi, S. Tsutsumi, N. Machida, J. M. Chong, M. Fukayama, T. Kodama, and H. Aburatani.** 2002. Global gene expression analysis of gastric cancer by oligonucleotide microarrays. Cancer Res. **62:**233–240.
53. **Hirota, S., K. Isozaki, Y. Moriyama, K. Hashimoto, T. Nishida, S. Ishiguro, K. Kawano, M. Hanada, A. Kurata, M. Takeda, G. Muhammad Tunio, Y. Matsuzawa, Y. Kanakura, Y. Shinomura, and Y. Kitamura.** 1998. Gain-of-function mutations of c-kit in human gastrointestinal stromal tumors. Science **279:**577–580.
54. **Hoeflich, A., R. Reisinger, H. Lahm, W. Kiess, W. F. Blum, H. J. Kolb, M. M. Weber, and E. Wolf.** 2001. Insulin-like growth factor-binding protein 2 in tumorigenesis: protector or promoter? Cancer Res. **61:**8601–8610.
55. **Ihara, H., T. Urano, A. Takada, and D. J. Loskutoff.** 2001. Induction of plasminogen activator inhibitor 1 gene expression in adipocytes by thiazolidinediones. FASEB J. **15:**1233–1235.
56. **Inoue, M., S. Kyo, M. Fujita, T. Enomoto, and G. Kondoh.** 1994. Coexpression of the c-kit receptor and the stem cell factor in gynecological tumors. Cancer Res. **54:**3049–3053.
57. **Jenner, R. G., M. M. Alba, C. Boshoff, and P. Kellam.**2001. Kaposi's

sarcoma-associated herpesvirus latent and lytic gene expression as revealed by DNA arrays. J. Virol. **75:**891–902.
58. **Krystal, G. W., S. J. Hines, and C. P. Organ.** 1996. Autocrine growth of small cell lung cancer mediated by coexpression of c-kit and stem cell factor. Cancer Res. **56:**370–376.
59. **Krystal, G. W., S. Honsawek, J. Litz, and E. Buchdunger.** 2000. The selective tyrosine kinase inhibitor STI571 inhibits small cell lung cancer growth. Clin. Cancer Res. **6:**3319–3326.
60. **Lagunoff, M., J. Bechtel, E. Venetsanakos, A. M. Roy, N. Abbey, B. Herndier, M. McMahon, and D. Ganem.** 2002. De novo infection and serial transmission of Kaposi's sarcoma-associated herpesvirus in cultured endothelial cells. J. Virol. **76:**2440–2448.
61. **Lev, S., Y. Yarden, and D. Givol.** 1990. Receptor functions and ligand-dependent transforming potential of a chimeric kit proto-oncogene. Mol. Cell. Biol. **10:**6064–6068.
62. **Li, J. J., Y. Q. Huang, C. J. Cockerell, and A. E. Friedman-Kien.** 1996. Localization of human herpes-like virus type 8 in vascular endothelial cells and perivascular spindle-shaped cells of Kaposi's sarcoma lesions by in situ hybridization. Am. J. Pathol. **148:**1741–1748.
63. **Linnekin, D.** 1999. Early signaling pathways activated by c-Kit in hematopoietic cells. Int. J. Biochem. Cell Biol. **31:**1053–1074.
64. **Liu, C., Y. Okruzhnov, H. Li, and J. Nicholas.** 2001. Human herpesvirus 8 (HHV-8)-encoded cytokines induce expression of and autocrine signaling by vascular endothelial growth factor (VEGF) in HHV-8-infected primary-effusion lymphoma cell lines and mediate VEGF-independent antiapoptotic effects. J. Virol. **75:**10933–10940.
65. **Lu, L., M. C. Heinrich, L. S. Wang, M. S. Dai, A. J. Zigler, L. Chai, and H. E. Broxmeyer.** 1999. Retroviral-mediated gene transduction of c-kit into single hematopoietic progenitor cells from cord blood enhances erythroid colony formation and decreases sensitivity to inhibition by tumor necrosis factor-alpha and transforming growth factor-β1. Blood **94:**2319–2332.
66. **Lux, M. L., B. P. Rubin, T. L. Biase, C. J. Chen, T. Maclure, G. Demetri, S. Xiao, S. Singer, C. D. Fletcher, and J. A. Fletcher.** 2000. KIT extracellular and kinase domain mutations in gastrointestinal stromal tumors. Am. J. Pathol. **156:**791–795.
67. **Martin, F. H., S. V. Suggs, K. E. Langley, H. S. Lu, J. Ting, K. H. Okino, C. F. Morris, I. K. McNiece, F. W. Jacobsen, E. A. Mendiaz, et al.** 1990. Primary structure and functional expression of rat and human stem cell factor DNAs. Cell **63:**203–211.
68. **Matsuda, R., T. Takahashi, S. Nakamura, Y. Sekido, K. Nishida, M. Seto, T. Seito, T. Sugiura, Y. Ariyoshi, et al.** 1993. Expression of the c-kit protein in human solid tumors and in corresponding fetal and adult normal tissues. Am. J. Pathol. **142:**339–346.
69. **Miettinen, M., M. Sarlomo-Rikala, and J. Lasota.** 2000. KIT expression in angiosarcomas and fetal endothelial cells: lack of mutations of exon 11 and exon 17 of C-kit. Mod. Pathol. **13:**536–541.
70. **Moore, P. S., C. Boshoff, R. A. Weiss, and Y. Chang.** 1996. Molecular mimicry of human cytokine and cytokine response pathway genes by KSHV. Science **274:**1739–1744.
71. **Moses, A. V., K. N. Fish, R. Ruhl, P. P. Smith, J. G. Strussenberg, L. Zhu, B. Chandran, and J. A. Nelson.** 1999. Long-term infection and transformation of dermal microvascular endothelial cells by human herpesvirus 8. J. Virol. **73:**6892–6902.
72. **Muller, W. A.** 2001. New mechanisms and pathways for monocyte recruitment. J. Exp. Med. **194:**F47–51.
73. **Muralidhar, S., A. M. Pumfery, M. Hassani, M. R. Sadaie, M. Kishishita, J. N. Brady, J. Doniger, P. Medveczky, and L. J. Rosenthal.** 1998. Identification of kaposin (open reading frame K12) as a human herpesvirus 8 (Kaposi's sarcoma-associated herpesvirus) transforming gene. J. Virol. **72:**4980–4988.
74. **Naeve, G. S., M. Ramakrishnan, R. Kramer, D. Hevroni, Y. Citri, and L. E. Theill.** 1997. Neuritin: a gene induced by neural activity and neurotrophins that promotes neuritogenesis. Proc. Natl. Acad. Sci. USA **94:**2648–2653.
75. **Nicholas, J., J. C. Zong, D. J. Alcendor, D. M. Ciufo, L. J. Poole, R. T. Sarisky, C. J. Chiou, X. Zhang, X. Wan, H. G. Guo, M. S. Reitz, and G. S. Hayward.** 1998. Novel organizational features, captured cellular genes, and strain variability within the genome of KSHV/HHV8. J. Natl. Cancer Inst. Monogr. **23:**79–88.
76. **Nishida, T., S. Hirota, M. Taniguchi, K. Hashimoto, K. Isozaki, H. Nakamura, Y. Kanakura, T. Tanaka, A. Takabayashi, H. Matsuda, and Y. Kitamura.** 1998. Familial gastrointestinal stromal tumours with germline mutation of the KIT gene. Nat Genet. **19:**323–324.
77. **Nomiyama, H., S. Fukuda, M. Iio, S. Tanase, R. Miura, and O. Yoshie.** 1999. Organization of the chemokine gene cluster on human chromosome 17q11.2 containing the genes for CC chemokine MPIF-1, HCC-2, HCC-1, LEC, and RANTES. J. Interferon Cytokine Res. **19:**227–234.
78. **Paulose-Murphy, M., N. K. Ha, C. Xiang, Y. Chen, L. Gillim, R. Yarchoan, P. Meltzer, M. Bittner, J. Trent, and S. Zeichner.** 2001. Transcription program of human herpesvirus 8 (Kaposi's sarcoma-associated herpesvirus). J. Virol. **75:**4843–4853.
79. **Pepper, M. S.** 2001. Extracellular proteolysis and angiogenesis. Thromb. Haemost. **86:**346–355.
80. **Poole, L. J., Y. Yu, P. S. Kim, Q. Z. Zheng, J. Pevsner, and G. S. Hayward.** 2002. Altered patterns of cellular gene expression in dermal microvascular endothelial cells infected with Kaposi's sarcoma-associated herpesvirus. J. Virol. **76:**3395–3420.
81. **Rabbitts, T. H., H. Axelson, A. Forster, G. Grutz, I. Lavenir, R. Larson, H. Osada, V. Valge-Archer, I. Wadman, and A. Warren.** 1997. Chromosomal translocations and leukaemia: a role for LMO2 in T cell acute leukaemia, in transcription and in erythropoiesis. Leukemia **11**(Suppl. 3)**:**271–272.
82. **Rainbow, L., G. M. Platt, G. R. Simpson, R. Sarid, S. J. Gao, H. Stoiber, C. S. Herrington, P. S. Moore, and T. F. Schulz.** 1997. The 222- to 234-kilodalton latent nuclear protein (LNA) of Kaposi's sarcoma-associated herpesvirus (human herpesvirus 8) is encoded by orf73 and is a component of the latency-associated nuclear antigen. J. Virol. **71:**5915–5921.
83. **Ramaswamy, S., P. Tamayo, R. Rifkin, S. Mukherjee, C. H. Yeang, M. Angelo, C. Ladd, M. Reich, E. Latulippe, J. P. Mesirov, T. Poggio, W. Gerald, M. Loda, E. S. Lander, and T. R. Golub.** 2001. Multiclass cancer diagnosis using tumor gene expression signatures. Proc. Natl. Acad. Sci. USA **98:**15149–15154.
84. **Renne, R., C. Barry, D. Dittmer, N. Compitello, P. O. Brown, and D. Ganem.** 2001. Modulation of cellular and viral gene expression by the latency-associated nuclear antigen of Kaposi's sarcoma-associated herpesvirus. J. Virol. **75:**458–468.
85. **Renne, R., D. Blackbourn, D. Whitby, J. Levy, and D. Ganem.** 1998. Limited transmission of Kaposi's sarcoma-associated herpesvirus in cultured cells. J. Virol. **72:**5182–5188.
86. **Renne, R., M. Lagunoff, W. Zhong, and D. Ganem.** 1996. The size and conformation of Kaposi's sarcoma-associated herpesvirus (human herpesvirus 8) DNA in infected cells and virions. J. Virol. **70:**8151–8154.
87. **Reul, B. A., L. N. Ongemba, A. M. Pottier, J. C. Henquin, and S. M. Brichard.** 1997. Insulin and insulin-like growth factor 1 antagonize the stimulation of ob gene expression by dexamethasone in cultured rat adipose tissue. Biochem. J. **324:**605–610.
88. **Roehm, N. W., G. H. Rodgers, S. M. Hatfield, and A. L. Glasebrook.** 1991. An improved colorimetric assay for cell proliferation and viability utilizing the tetrazolium salt XTT. J. Immunol. Methods **142:**257–265.
89. **Roth, W. K., H. Brandstetter, and M. Sturzl.** 1992. Cellular and molecular features of HIV-associated Kaposi's sarcoma. AIDS **6:**895–913. (Erratum, **6:**1411.)
90. **Roth, W. K., S. Werner, W. Risau, K. Remberger, and P. H. Hofschneider.** 1988. Cultured, AIDS-related Kaposi's sarcoma cells express endothelial cell markers and are weakly malignant in vitro. Int. J. Cancer **42:**767–773.
91. **Rutgers, J. L., R. Wieczorek, F. Bonetti, K. L. Kaplan, D. N. Posnett, A. E. Friedman-Kien, and D. M. Knowles II.** 1986. The expression of endothelial cell surface antigens by AIDS-associated Kaposi's sarcoma. Evidence for a vascular endothelial cell origin. Am. J. Pathol. **122:**493–499.
92. **Salunga, R. C., H. Guo, L. Luo, A. Bittner, K. C. Joy, J. R. Chambers, J. S. Wan, J. R. Jackson, and M. G. Erlander.** 1999. Gene expression analysis via cDNA microarrays of laser capture microdissected cells from fixed tissue, p. 121–136. *In* M. Schena (ed.), DNA microarrays. A practical approach. Oxford Press, Oxford, United Kingdom.
93. **Sarid, R., O. Flore, R. A. Bohenzky, Y. Chang, and P. S. Moore.** 1998. Transcription mapping of the Kaposi's sarcoma-associated herpesvirus (human herpesvirus 8) genome in a body cavity-based lymphoma cell line (BC-1). J. Virol. **72:**1005–1012.
94. **Sciacca, F. L., M. Stuerzl, F. Bussolino, M. Sironi, H. Brandstetter, C. Zietz, D. Zhou, C. Matteucci, G. Peri, et al.** 1994. Expression of adhesion molecules, platelet-activating factor, and chemokines by Kaposi's sarcoma cells. J. Immunol. **153:**4816–4825.
95. **Scott, R. S., E. J. McMahon, S. M. Pop, E. A. Reap, R. Caricchio, P. L. Cohen, H. S. Earp, and G. K. Matsushima.** 2001. Phagocytosis and clearance of apoptotic cells is mediated by MER. Nature **411:**207–211.
96. **Scully, P. A., H. K. Steinman, C. Kennedy, K. Trueblood, D. M. Frisman, and J. R. Voland.** 1988. AIDS-related Kaposi's sarcoma displays differential expression of endothelial surface antigens. Am. J. Pathol. **130:**244–251.
97. **Simmen, K. A., J. Singh, B. G. Luukkonen, M. Lopper, A. Bittner, N. E. Miller, M. R. Jackson, T. Compton, and K. Fruh.** 2001. Global modulation of cellular transcription by human cytomegalovirus is initiated by viral glycoprotein B. Proc. Natl. Acad. Sci. USA **98:**7140–7145.
98. **Sodhi, A., S. Montaner, V. Patel, M. Zohar, C. Bais, E. A. Mesri, and J. S. Gutkind.** 2000. The Kaposi's sarcoma-associated herpes virus G protein-coupled receptor up-regulates vascular endothelial growth factor expression and secretion through mitogen-activated protein kinase and p38 pathways acting on hypoxia-inducible factor 1α. Cancer Res. **60:**4873–4880.
99. **Staskus, K. A., R. Sun, G. Miller, P. Racz, A. Jaslowski, C. Metroka, H. Brett-Smith, and A. T. Haase.** 1999. Cellular tropism and viral interleukin-6 expression distinguish human herpesvirus 8 involvement in Kaposi's sarcoma, primary effusion lymphoma, and multicentric Castleman's disease. J. Virol. **73:**4181–4187.
100. **Staskus, K. A., W. Zhong, K. Gebhard, B. Herndier, H. Wang, R. Renne, J. Beneke, J. Pudney, D. J. Anderson, D. Ganem, and A. T. Haase.** 1997. Kaposi's sarcoma-associated herpesvirus gene expression in endothelial (spindle) tumor cells. J. Virol. **71:**715–719.

101. **Streblow, D. N., C. Soderberg-Naucler, J. Vieira, P. Smith, E. Wakabayashi, F. Ruchti, K. Mattison, Y. Altschuler, and J. A. Nelson.** 1999. The human cytomegalovirus chemokine receptor US28 mediates vascular smooth muscle cell migration. Cell **99:**511–520.
102. **Sturzl, M., C. Blasig, A. Schreier, F. Neipel, C. Hohenadl, E. Cornali, G. Ascherl, S. Esser, N. H. Brockmeyer, M. Ekman, E. E. Kaaya, E. Tschachler, and P. Biberfeld.** 1997. Expression of HHV-8 latency-associated T0.7 RNA in spindle cells and endothelial cells of AIDS-associated, classical and African Kaposi's sarcoma. Int. J. Cancer **72:**68–71.
103. **Sun, R., S. F. Lin, K. Staskus, L. Gradoville, E. Grogan, A. Haase, and G. Miller.** 1999. Kinetics of Kaposi's sarcoma-associated herpesvirus gene expression. J. Virol. **73:**2232–2242.
104. **Swanton, C., D. J. Mann, B. Fleckenstein, F. Neipel, G. Peters, and N. Jones.** 1997. Herpes viral cyclin/Cdk6 complexes evade inhibition by CDK inhibitor proteins. Nature **390:**184–187.
105. **Taraboletti, G., R. Benelli, P. Borsotti, M. Rusnati, M. Presta, R. Giavazzi, L. Ruco, and A. Albini.** 1999. Thrombospondin-1 inhibits Kaposi's sarcoma (KS) cell and HIV-1 Tat-induced angiogenesis and is poorly expressed in KS lesions. J. Pathol. **188:**76–81.
106. **Thome, M., P. Schneider, K. Hofmann, H. Fickenscher, E. Meinl, F. Neipel, C. Mattmann, K. Burns, J. L. Bodmer, M. Schroter, C. Scaffidi, P. H. Krammer, M. E. Peter, and J. Tschopp.** 1997. Viral FLICE-inhibitory proteins (FLIPs) prevent apoptosis induced by death receptors. Nature **386:**517–521.
107. **Tian, Q., H. F. Frierson, Jr., G. W. Krystal, and C. A. Moskaluk.** 1999. Activating c-kit gene mutations in human germ cell tumors. Am. J. Pathol. **154:**1643–1647.
108. **Tontonoz, P., L. Nagy, J. G. Alvarez, V. A. Thomazy, and R. M. Evans.** 1998. PPARgamma promotes monocyte/macrophage differentiation and uptake of oxidized LDL. Cell **93:**241–252.
109. **Turner, A. M., K. M. Zsebo, F. Martin, F. W. Jacobsen, L. G. Bennett, and V. C. Broudy.** 1992. Nonhematopoietic tumor cell lines express stem cell factor and display c-kit receptors. Blood **80:**374–381.
110. **Vieira, J., P. O'Hearn, L. Kimball, B. Chandran, and L. Corey.** 2001. Activation of Kaposi's sarcoma-associated herpesvirus (human herpesvirus 8) lytic replication by human cytomegalovirus. J. Virol. **75:**1378–1386.
111. **Wang, W. L., M. E. Healy, M. Sattler, S. Verma, J. Lin, G. Maulik, C. D. Stiles, J. D. Griffin, B. E. Johnson, and R. Salgia.** 2000. Growth inhibition and modulation of kinase pathways of small cell lung cancer cell lines by the novel tyrosine kinase inhibitor STI 571. Oncogene **19:**3521–3528.
112. **Yamada, Y., R. Pannell, A. Forster, and T. H. Rabbitts.** 2000. The oncogenic LIM-only transcription factor Lmo2 regulates angiogenesis but not vasculogenesis in mice. Proc. Natl. Acad. Sci. USA **97:**320–324.
113. **Yamaguchi, H., E. Ishii, S. Saito, K. Tashiro, I. Fujita, S. Yoshidomi, M. Ohtubo, K. Akazawa, and S. Miyazaki.** 1996. Umbilical vein endothelial cells are an important source of c-kit and stem cell factor which regulate the proliferation of haemopoietic progenitor cells. Br. J. Haematol. **94:**606–611.
114. **Yarden, Y., W. J. Kuang, T. Yang-Feng, L. Coussens, S. Munemitsu, T. J. Dull, E. Chen, J. Schlessinger, U. Francke, and A. Ullrich.** 1987. Human proto-oncogene c-kit: a new cell surface receptor tyrosine kinase for an unidentified ligand. EMBO J. **6:**3341–3351.
115. **Zhao, B., R. A. Bowden, S. A. Stavchansky, and P. D. Bowman.** 2001. Human endothelial cell response to gram-negative lipopolysaccharide assessed with cDNA microarrays. Am. J. Physiol. Cell Physiol. **281:**C1587–C1595.
116. **Zhong, W., H. Wang, B. Herndier, and D. Ganem.** 1996. Restricted expression of Kaposi sarcoma-associated herpesvirus (human herpesvirus 8) genes in Kaposi sarcoma. Proc. Natl. Acad. Sci. USA **93:**6641–6646.